Astrofisica Nucleare e Subnucleare

“MeV” Astrophysics

Coded Mask Imaging

The Coded Mask Technique

is the worst possible way of making a telescope

Except when you can 't do anything better !

- Wide fields of view
- Energies too high for focussing, or too low for Compton/Tracking detector techniques
- Very good angular resolution
- The best energy resolution

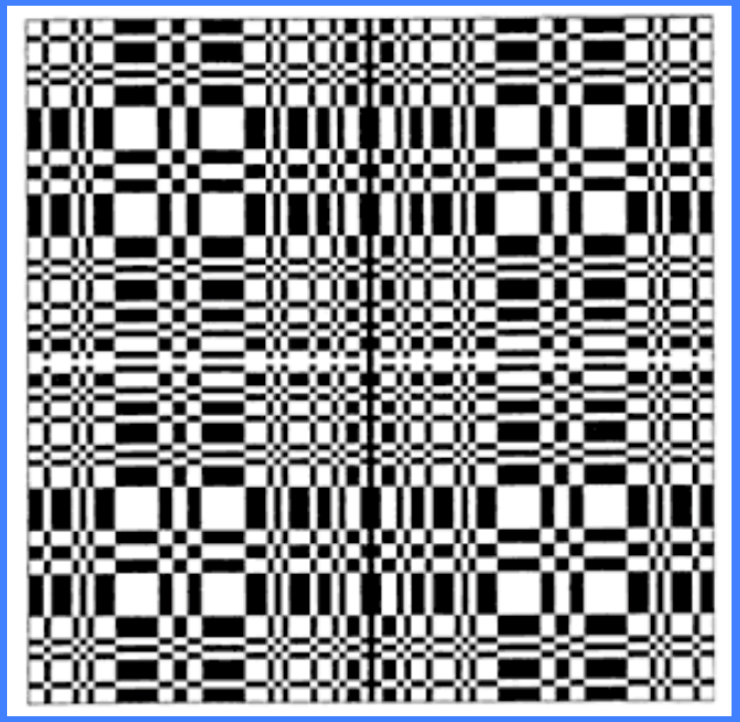

Mask of IBIS (15 keV – 10 MeV)
onboard *INTEGRAL*

Coded Mask Imaging

The Coded Masks for Integral

JEM-X

Energy: 3-100 keV
535mm dia
0.5mm Tungsten
3.3 mm pitch
Resolution 3 arc min

IBIS

Energy: 15-10000 keV
1064 mm square
16 mm Tungsten
11.2 mm pitch
Resolution 12 arc min

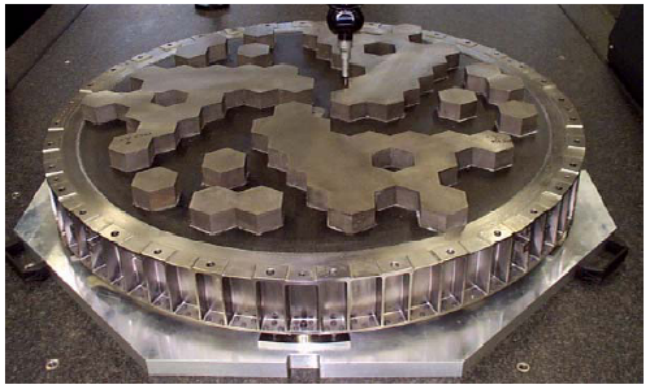

SPI

Energy: 20-8000 keV
770 mm dia
3 cm thick Tungsten
60 mm pitch
Resolution ~ 2.5°

INTEGRAL

INTEGRAL, the International Gamma-Ray Astrophysics Laboratory
Fine spectroscopy (E/dE=500) and fine imaging (angular resolution of 12' FWHM)
Energy range 15 keV to 10 MeV
plus simultaneous X-ray (3-35 keV) and optical (550 nm) monitoring capability
Two main g-ray instruments: SPI (spectroscopy) and IBIS (imager)

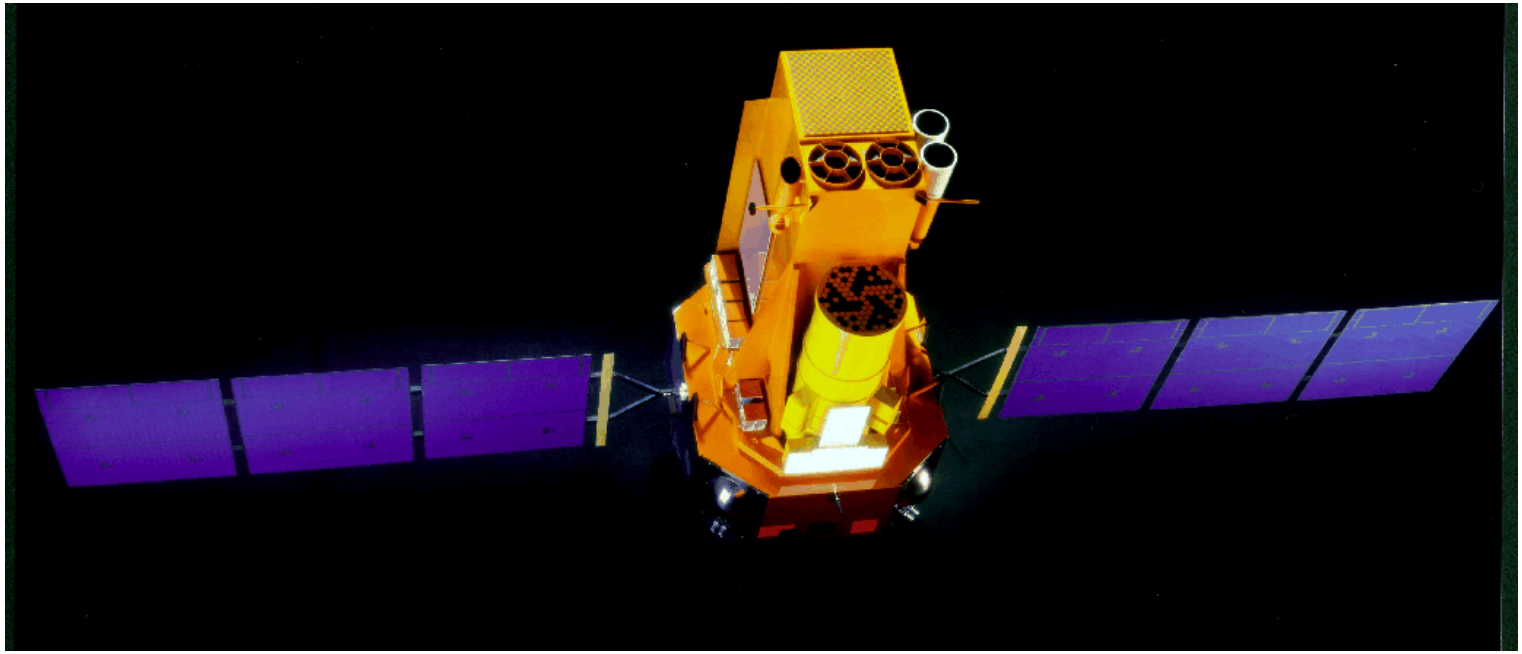

http://integral.esa.int

INTEGRAL

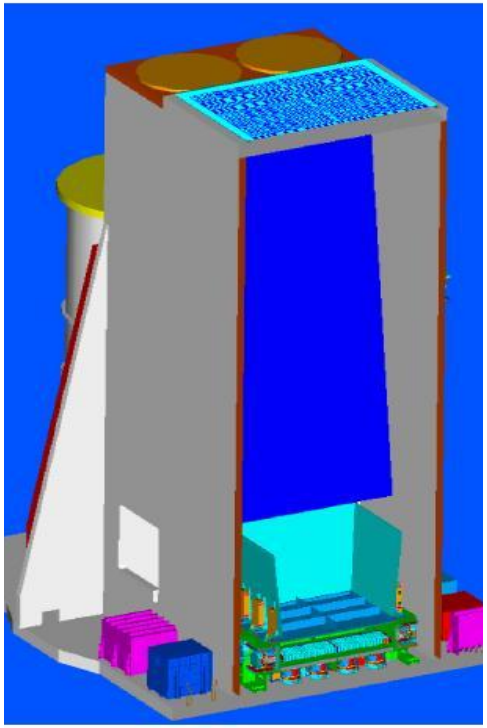

Imager IBIS

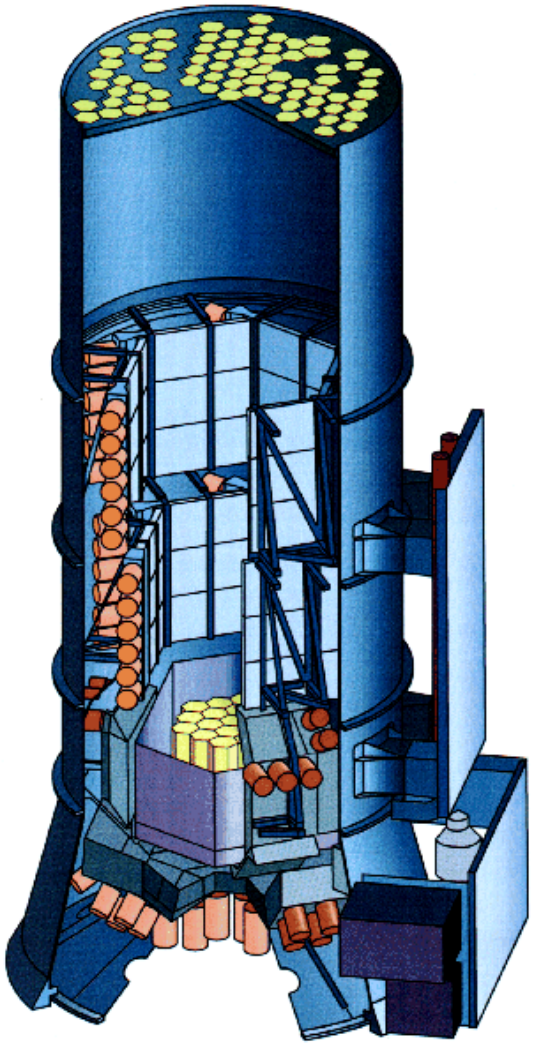

Spectrometer SPI

IBIS

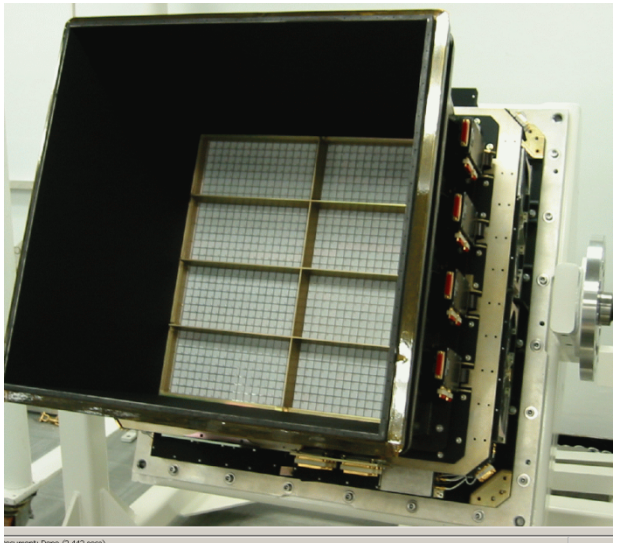

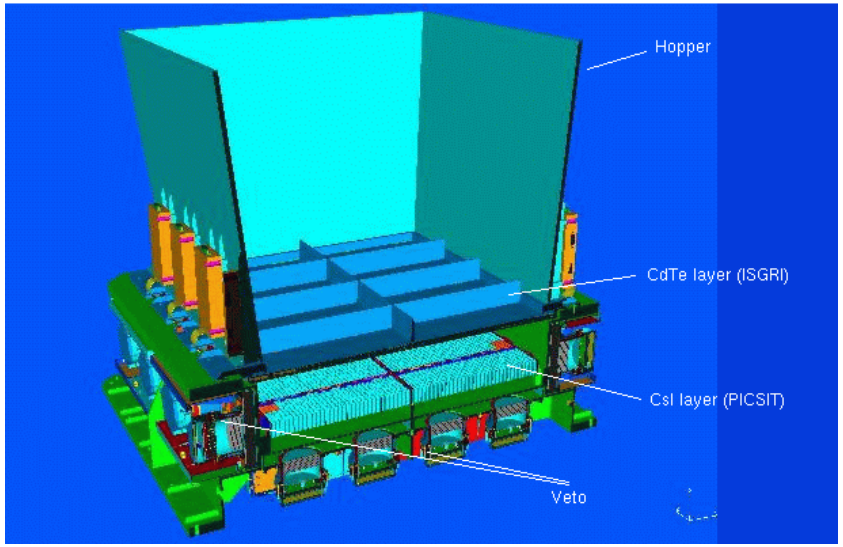

The Imager IBIS (Imager on Board the Integral Satellite) provides diagnostic capabilities of fine imaging (12 arcmin FWHM), source identification and spectral sensitivity to both continuum and broad lines over a broad (15 keV - 10 MeV) energy range. The Imager will exploit simultanesously with the other instruments on Integral celestial objects of all classes ranging from the most compact galactic systems to extragalactic objects.
A tungsten coded-aperture mask (located at 3.2 m above the detection plane) is optimised for high angular resolution. As diffraction is negligible at gamma-ray wavelengths, the angular resolution obtainable with a coded mask telescope is limited by the spatial resolution of the detector array. The Imager design takes advantage of this by utilising a detector with a large number of spatially resolved pixels, implemented as physically distinct elements.
The detector uses two planes, one 2600 cm^2 front layer of CdTe pixels, each (4x4x2) mm (width x depth x height), and a 3000 cm^2 layer of CsI pixels, each (9x9x30) mm. The CdTe array (ISGRI) and the CsI array (PICsIT) are separated by 90 mm. The detector provides the wide energy range and high sensitivity continuum spectroscopy required for Integral. The division into two layers allows the paths of the photons to be tracked in 3D, as they scatter and interact with more than one element. Events can be categorised and the signal to noise ratio improved by rejecting those which are unlikely to correspond to real (celestial) photons, e.g. towards the high end of the energy range.
The aperture is restricted by a lead shielding tube and shielded in all other directions by an active BGO scintillator veto.

SPI

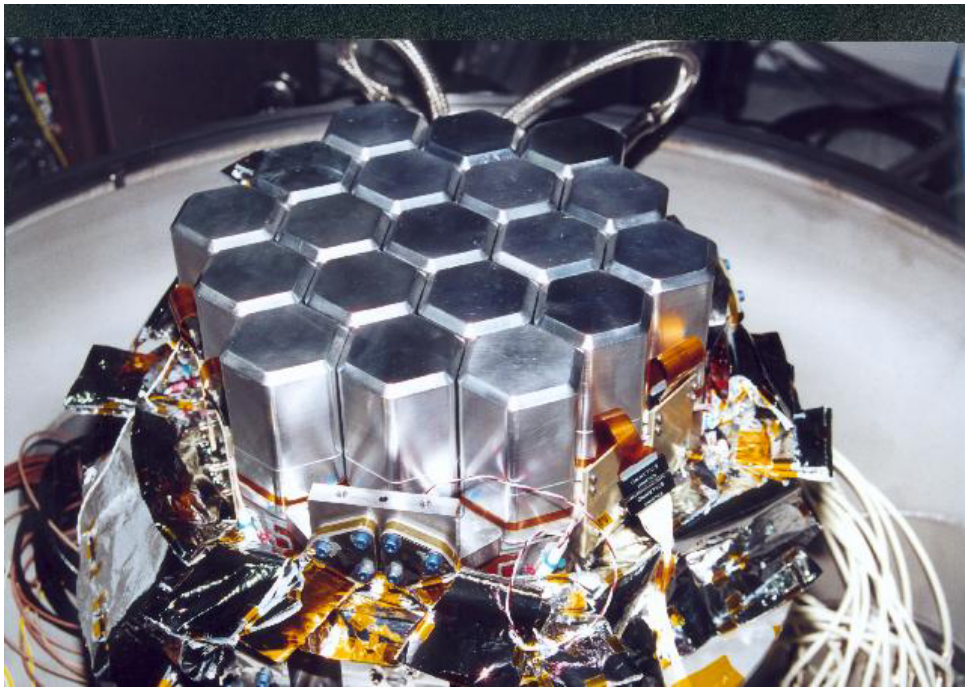

The spectrometer SPI (SPectrometer on INTEGRAL) will perform spectral analysis of gamma-ray point sources and extended regions in the 18 keV - 8 MeV energy range with an energy resolution of 2.2 keV (FWHM) at 1.33 MeV. This will be accomplished using an array of 19 hexagonal high purity Germanium detectors cooled by a Stirling cooler system to an operating temperature of 85 K. A hexagonal coded aperture mask is located 1.7 m above the detection plane in order to image large regions of the sky (fully coded field of view = 16 degrees) with an angular resolution of 2.5 degrees. In order to reduce background radiation, the detector assembly is shielded by a veto (anticoincidence) system which extends around the bottom and side of the detector almost completely up to the coded mask. The aperture (and hence contribution by cosmic diffuse radiation) is limited to ~ 30 degr. A plastic veto is provided below the mask to further reduce the 511 keV background.

Gamma Spectroscopy

Gammaray astronomy - Germanium detectors

Available as either:

PLANAR devices

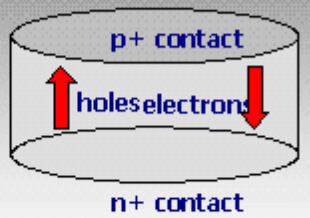

or COAXIAL

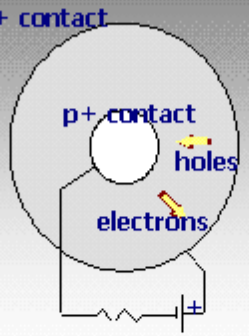

PLANAR Better at low energies
Limited size & stopping power

COAXIAL Slightly poorer resolution
Much larger

BOTH Ultimate in spectral resolution
Must be cooled to ~70K in use
May be arrayed to build an imaging detector

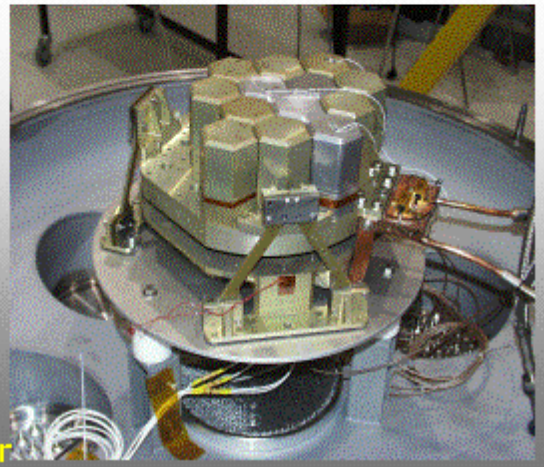

SPI @ INTEGRAL – a Ge spectrometer

Gamma Spectroscopy

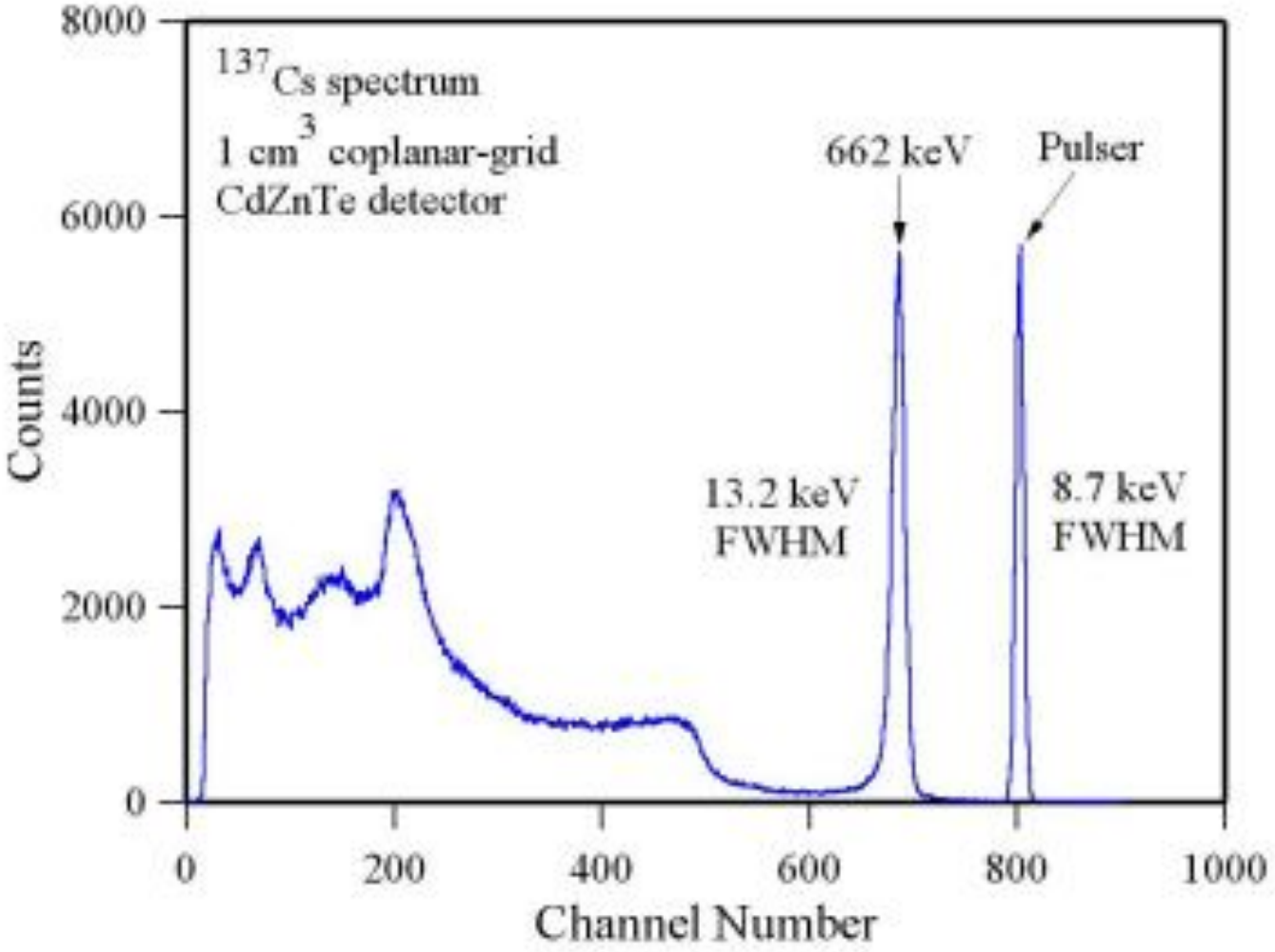

Rivelatori al Germanio

· Good response to high-energy photons

• Germanium is the best choice for high-energy (E > 100 keV – 10 MeV) spectroscopy

Very thin surface dead layers may give Ge an advantage where response from 1 keV - 100's of keV is desired

• Disadvantages (compared to compound semiconductors or scintillation detectors)

Requires cooling (complexity and cost)
Surfaces sensitive to contamination (handling/packaging more difficult)
For fine (Dx < 1 mm) position-sensitive detectors, segmented contact technology not well developed.

Examples CdTe: *Integral*/IBIS (SPI)

Rivelatori a stato solido a temperatura ambiente: Cd(Zn)Te – Cadmium Zinc Telluride (CZT)

- **Energy gap (1.4-2.2 eV)**
  - **Non necessaria criogenia (a differenza del Ge)**
- **Alta ρ (~6 g cm^{-3}) per massimizzare l'efficienza**
- **Alto Z (48, 52) per effetto fotoelettrico:**
  - **10 volte il μ_{Compt} fino a 110 keV (60 il Ge, 25 il Si);**
  - **Single site ok per imaging**
- **Facilmente segmentabile a piccole dimensioni:**
  - **$\Rightarrow$ risoluzione spaziale**

Examples CdTe: *Integral*/IBIS (ISGRI) – *Swift*/BAT

INTEGRAL

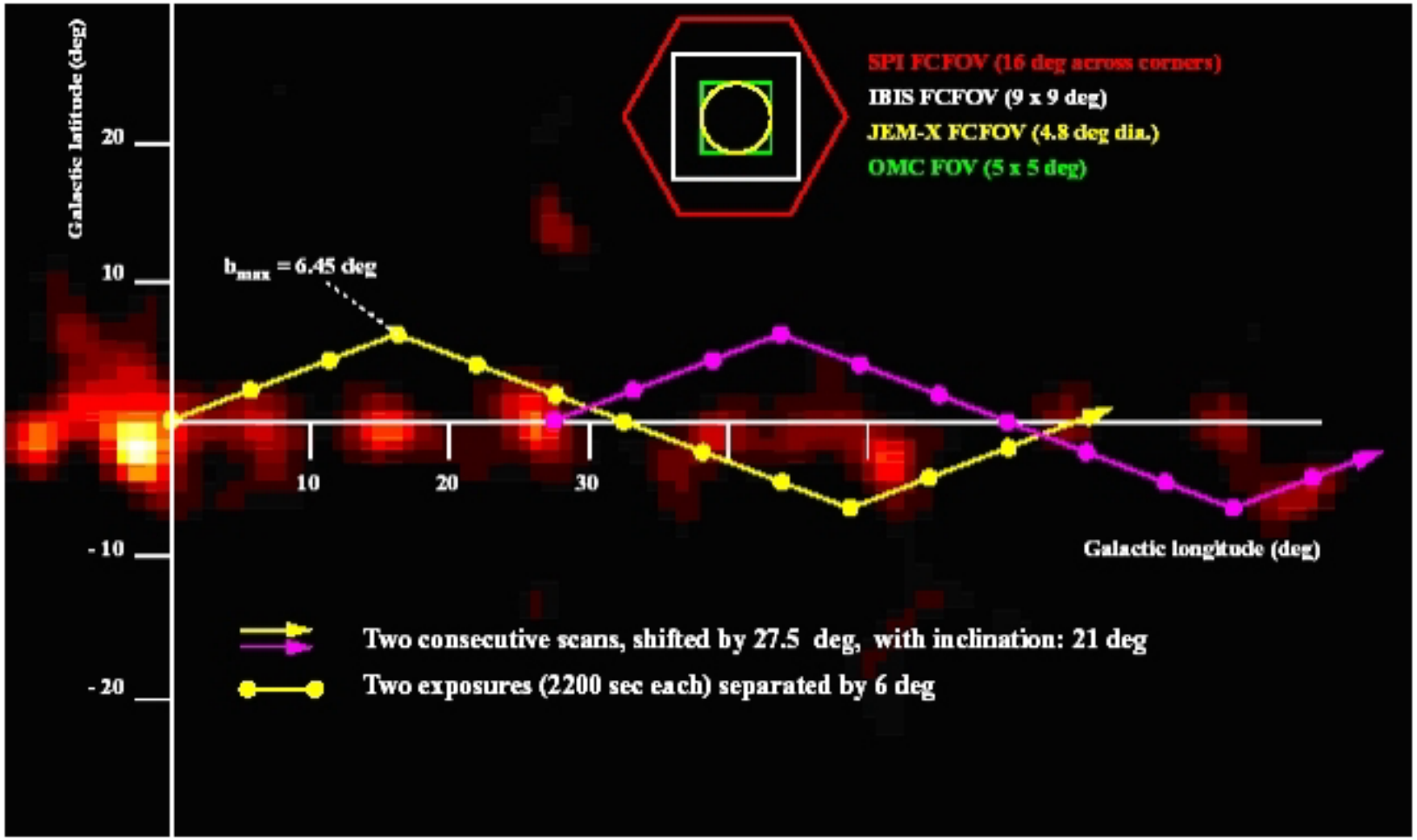
Galactic latitude (deg)
20
10
- 10
- 20
b_{max} = 6.45 deg
10
20
30
Galactic longitude (deg)
SPI FCFOV (16 deg across corners)
IBIS FCFOV (9 x 9 deg)
JEM-X FCFOV (4.8 deg dia.)
OMC FOV (5 x 5 deg)
Two consecutive scans, shifted by 27.5 deg, with inclination: 21 deg
Two exposures (2200 sec each) separated by 6 deg

INTEGRAL

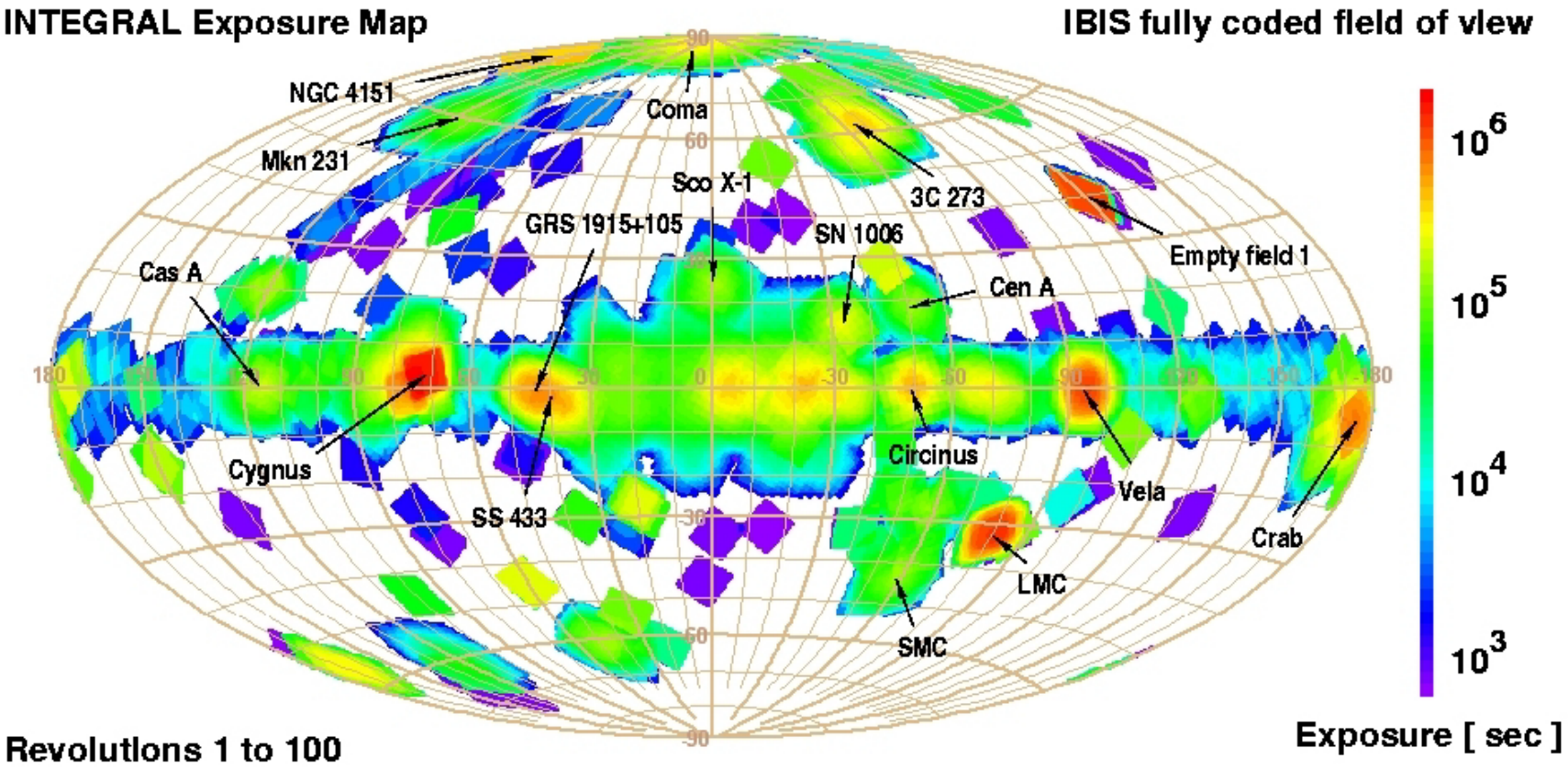
INTEGRAL Exposure Map
IBIS fully coded field of view
NGC 4151
Coma
Mkn 231
Sco X-1
3C 273
GRS 1915+105
SN 1006
Empty field 1
Cas A
Cen A
Cygnus
Circinus
Vela
SS 433
Crab
LMC
SMC
10^6
10^5
10^4
10^3
Exposure [sec]
Revolutions 1 to 100

INTEGRAL

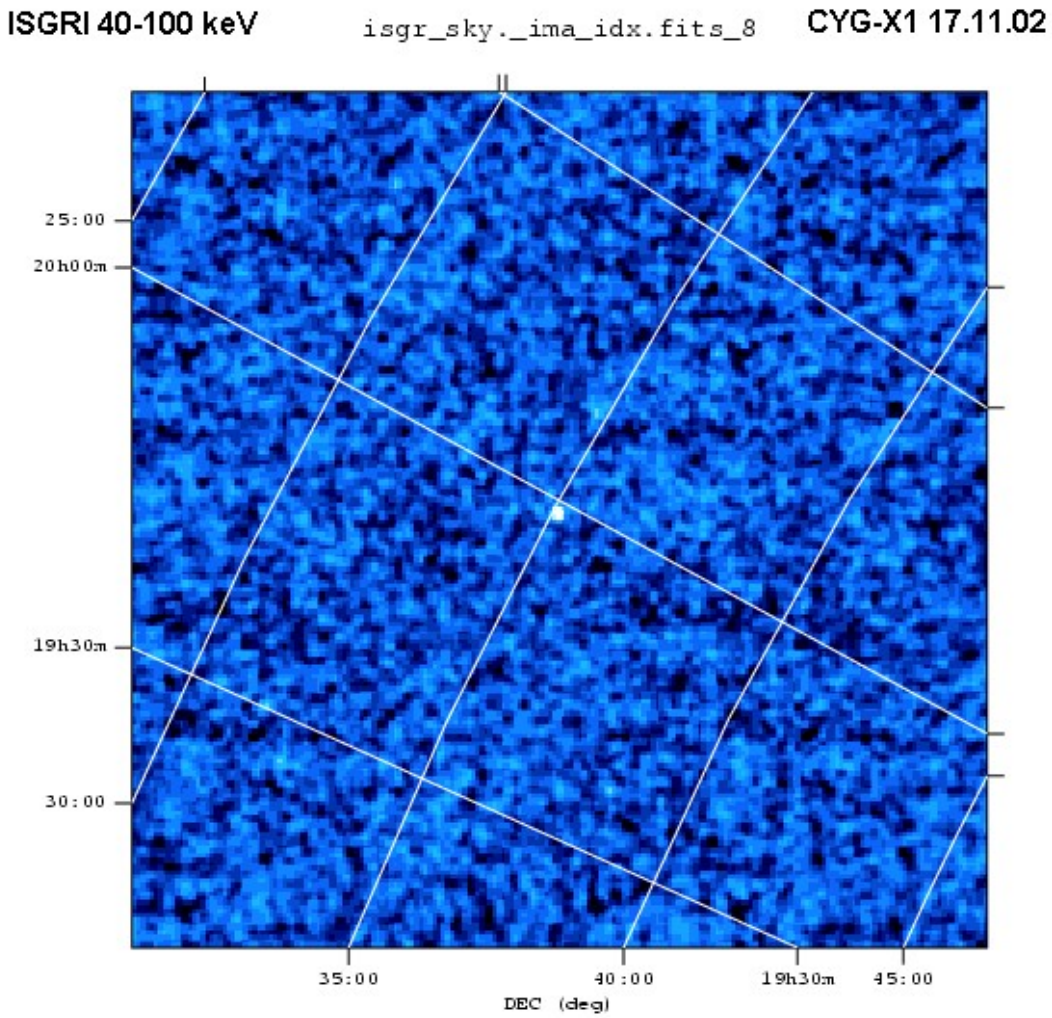
ISGRI 40-100 keV
isgr_sky._ima_idx.fits_8
CYG-X1 17.11.02
25:00
20h00m
19h30m
30:00
35:00
40:00
19h30m
45:00
DEC (deg)

INTEGRAL Science Objectives

Outline INTEGRAL Science Objectives

The scientific goals of Integral are addressed through the use of high resolution spectroscopy with fine imaging and accurate positioning of celestial sources in the gamma-ray domain. The following list of topics will be addressed by Integral:

- Compact Objects *(White Dwarfs, Neutron Stars, Black Hole Candidates, High Energy Transients and Gamma-Ray Bursts)*
- Extragalactic Astronomy *(Galaxies, Clusters, AGN, Seyferts, Blazars, Cosmic Diffuse Background)*
- Stellar Nucleosynthesis *(Hydrostatic Nucleosynthesis (AGB, WR Stars), Explosive Nucleosynthesis (Supernovae, Novae))*
- Galactic Structure *(Cloud Complex Regions, Mapping of continuum and line emission, ISM, CR distribution)*
- The Galactic Centre
- Particle Processes and Acceleration *(Transrelativistic Pair Plasmas, Beams, Jets)*
- Identification of High Energy Sources *(Unidentified Gamma-Ray Objects as a Class)*
- PLUS: Unexpected Discoveries

Gamma-Ray Astrophysics before INTEGRAL

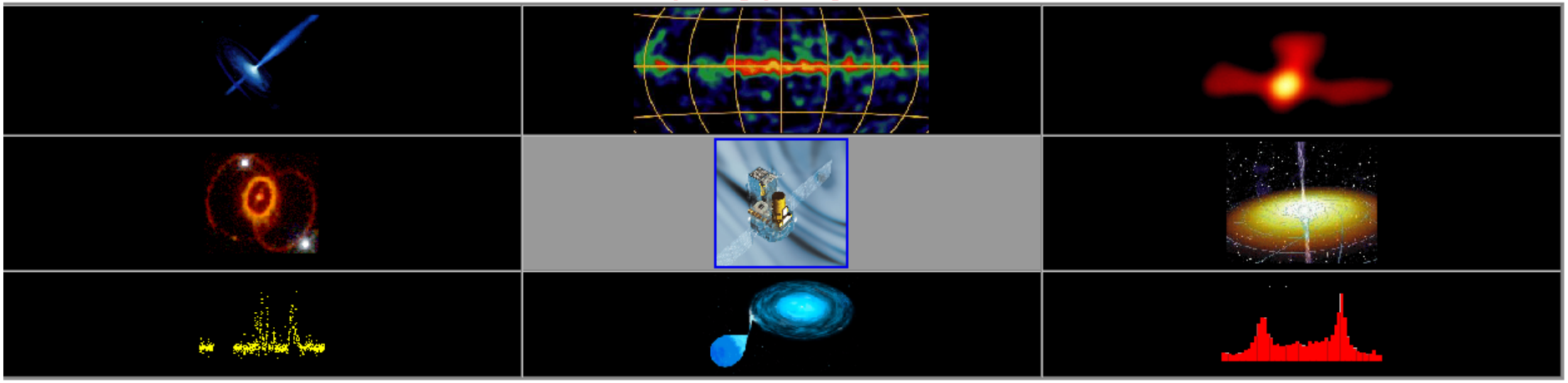

INTEGRAL

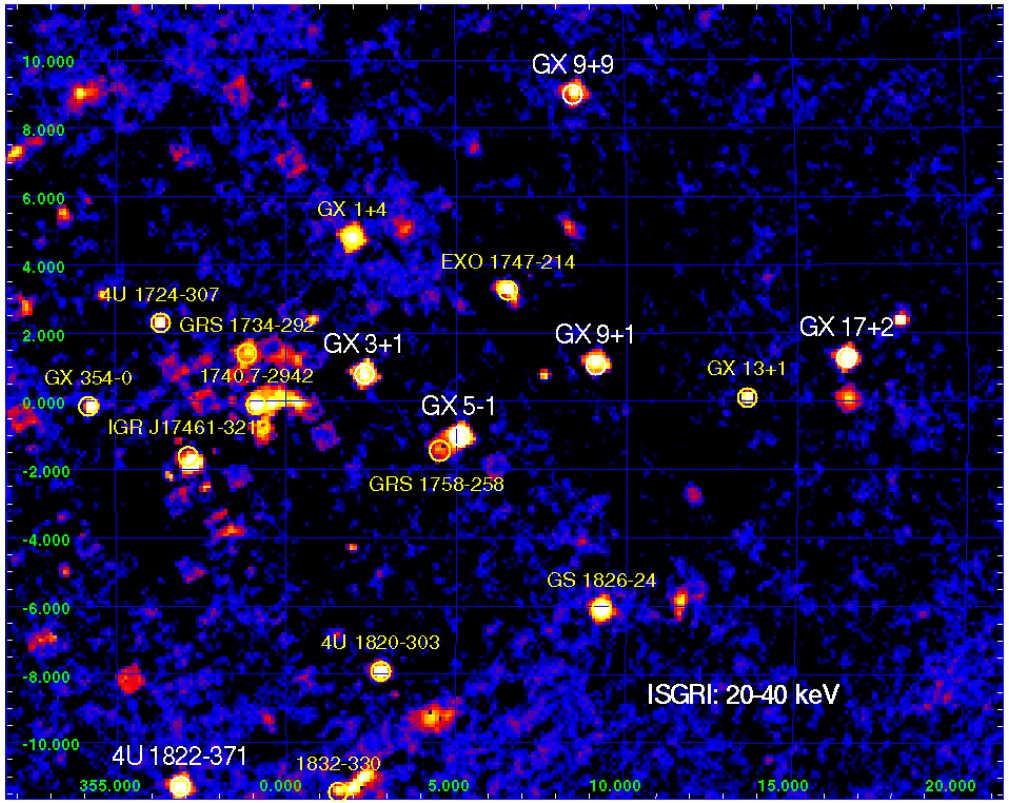

The image is an IBIS/ISGRI image of the Galactic Centre in the 20-40 keV band.
The analysis of IBIS/ISGRI data is based on GCDE
(Galactic Center Deep Exposure) and GPS (Galactic Plane Scan) data from revolution 30 to 64 i.e. January 11th to April 22nd, 2003 for a total of one thousand pointings (about 2 Msec exposure)

INTEGRAL

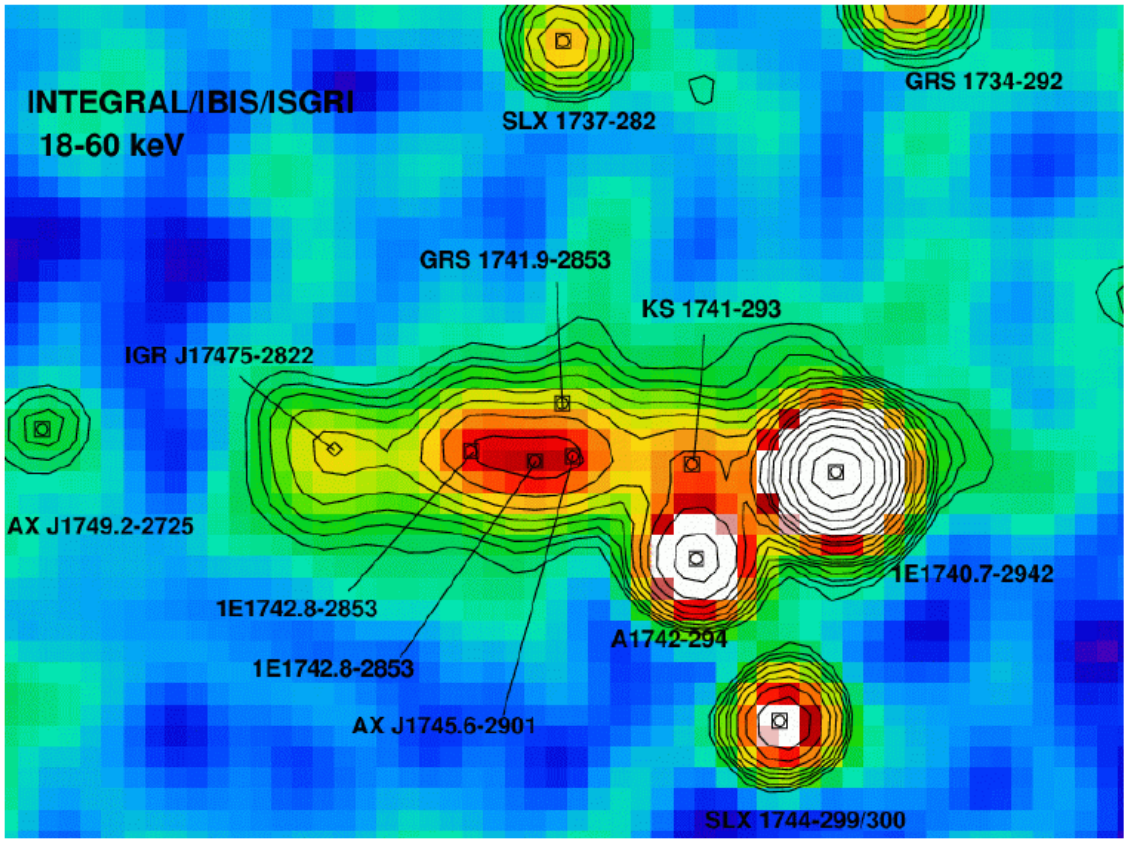

INTEGRAL views a Compton mirror at the Galactic Centre. M. Revnivtsev et al. report on the association of IGR J17475-2822, recently discovered by INTEGRAL, with the giant molecular cloud Sgr B2 in the Galactic Center region. Data from different observatories strongly support the idea that the hard X-ray emission of Sgr B2 is Compton scattered and reprocessed radiation emitted in the past by the Sgr A* source, the supermassive black-hole candidate in the center of our Galaxy. The IBIS/ISGRI image (18-60 keV) shows the inner 3.5 degree by 2.5 degree region of the center of the Galaxy. Contours represent signal-to-noise levels starting at S/N = 5 and increasing with a factor 1.4. The image has a total effective exposure time of 2.3 Ms.

INTEGRAL

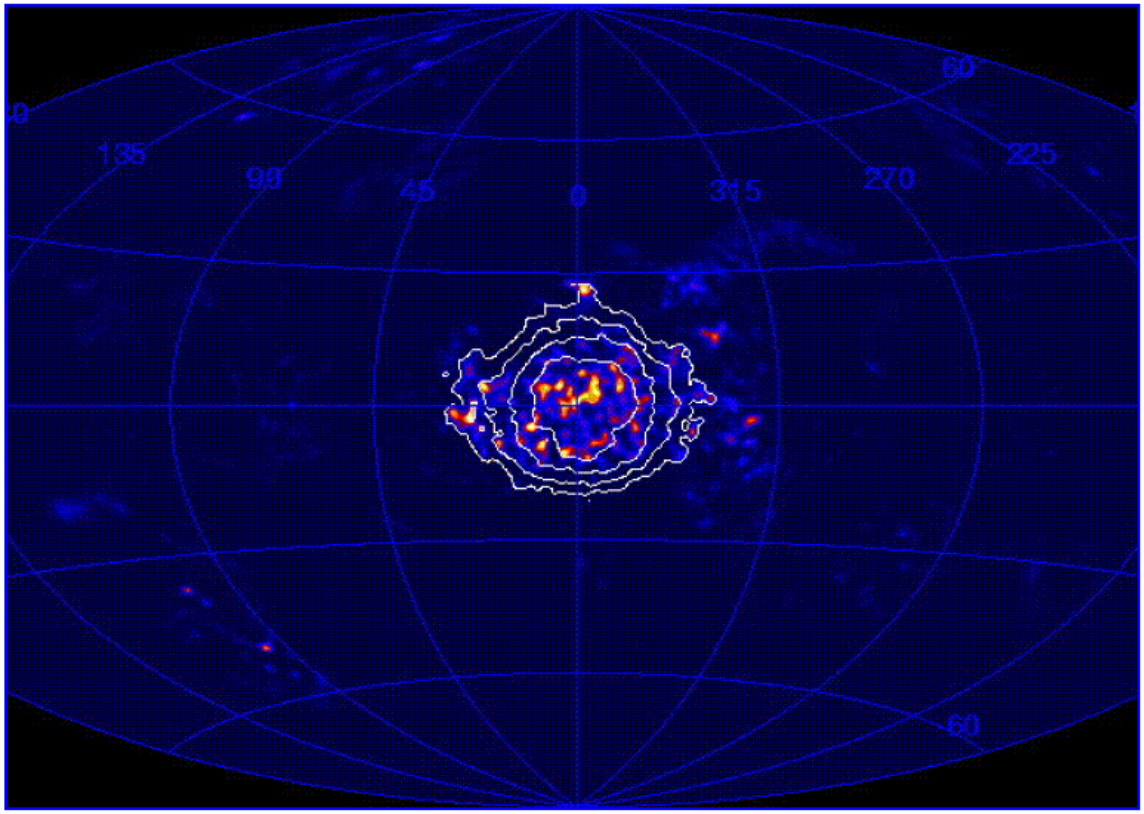

The SPI instrument onboard INTEGRAL has performed a search for 511 keV emission (resulting from positron-electron annihilation) all over the sky. The figure represents the results of this search: the all-sky map in galactic co-ordinates shows that 511 keV emission is - so far - only seen towards the center of our Galaxy. The SPI data are equally compatible with galactic bulge or halo distributions, the combination of a bulge and a disk component, or a combination of a number of point sources. Such distributions are expected if positrons originate either from low-mass X-ray binaries, novae, Type Ia supernovae, or possibly light dark matter.

INTEGRAL

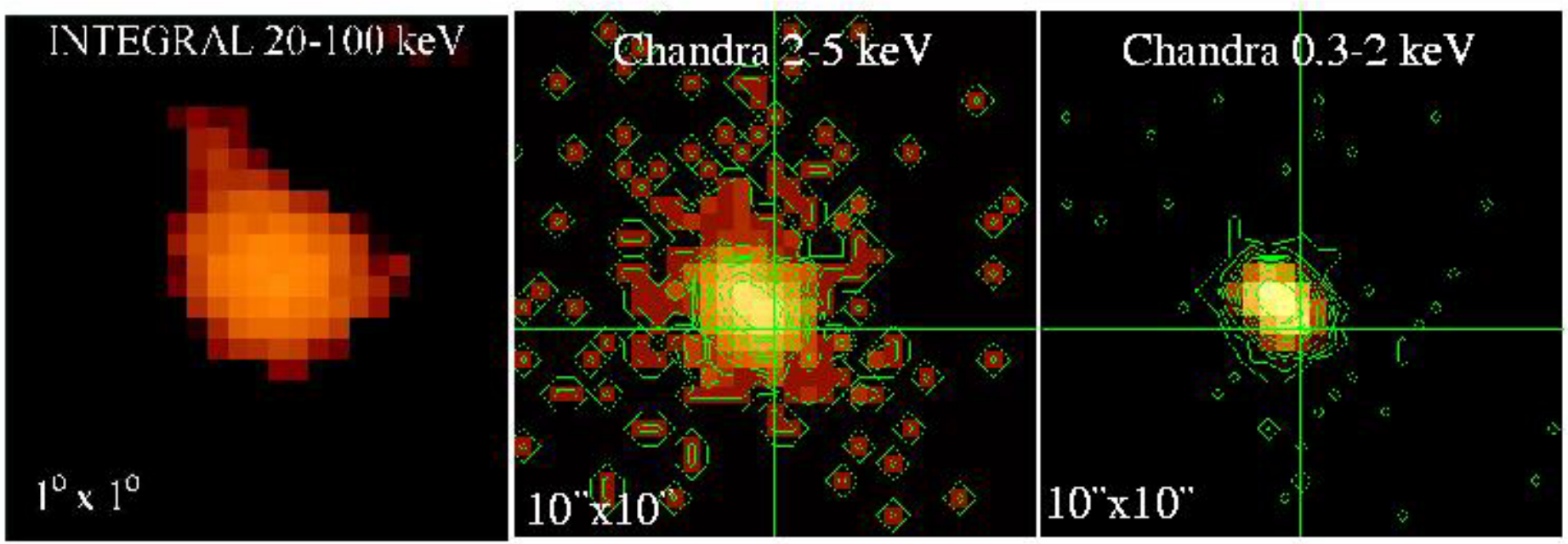

The blazar PKS 1830-211 is one of the most distant objects observed so far by INTEGRAL, it was reported as an ISGRI source in the galactic centre region. The source is clearly detected in 20-100 keV band. The image from IBIS/ISGRI is shown in the left panel. Notwithstanding its high redshift (z=2.507) it is a bright X-ray source, due to gravitational lensing by an intervening galaxy at z=0.89. Radio observations show two compact components separated by about 1 arcsecond; this effect (just at the limit of the angular resolution of Chandra), is clearly visible in the elliptically shaped Chandra images (central and right panels).

By assuming a magnification factor due to the lensing of the order of 10, the bolometric luminosity of PKS 1830-211 is huge: about 10^48 erg/s! The spectrum can be modelled adding an external source of low energy photons scattered up to gamma-ray energies by relativistic electrons. As observed in some high redshift quasars, Chandra spectra of PKS 1830-211 show evidence of absorption below 5 keV (rest frame). This effect could be due either to the lens galaxy at z=0.89 or to an intrinsic warm (ionized) gas at redshift of the source.

INTEGRAL

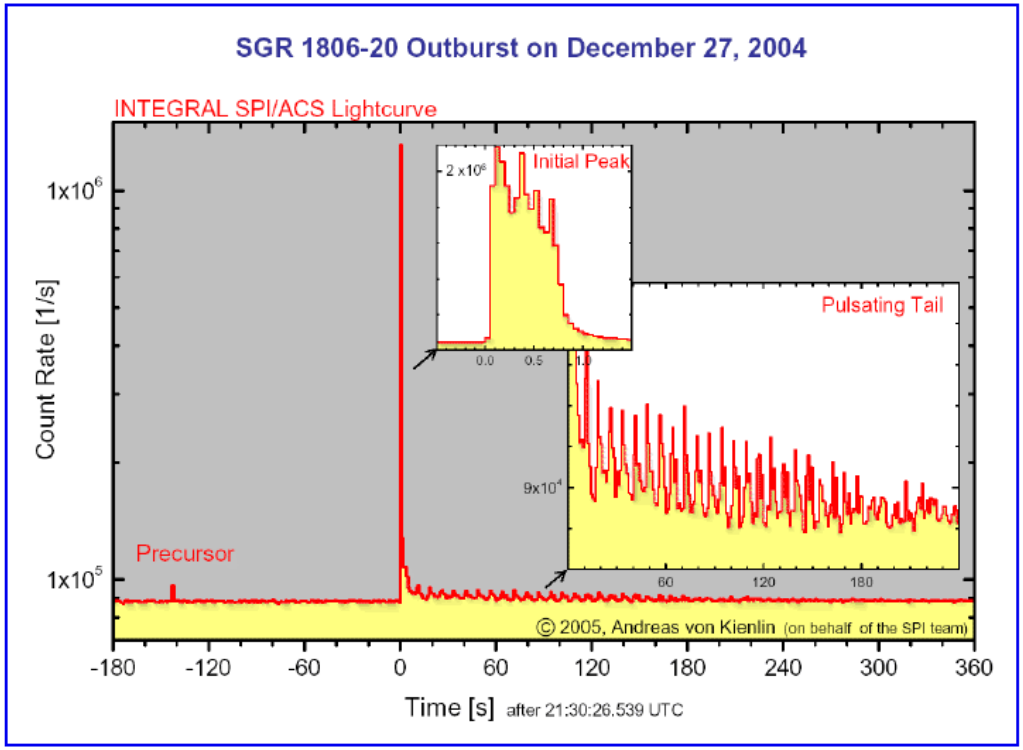

SGR 1806-20 which belongs to the class of soft gamma-ray repeaters (SGR) is believed to be a rotating neutron star with a super-strong magnetic field (10^15 Gauss); a so-called magnetar. The tremendous outburst of SGR 1806-20 on December 27, 2004 as seen by the large anticoincidence shield (ACS) of the INTEGRAL-spectrometer SPI is shown in the figure. The mean veto count rate of the ACS (~88000 counts/s) is interrupted at 21:30:26.539 UTC (T=0) by a steep count-rate increase (about a factor 25) for about 0.7 s. This outburst is thought to be caused by a large-scale rearrangement to a state of lower energy of a magnetar's super-strong magnetic field (10^15 Gauss), which is the current model for soft gamma-ray repeaters. The ~300 s long pulsating tail with a period of 7.56 s is clearly seen and can be explained by a trapped fireball which is co-rotating with the neutron star (magnetar).
The initial peak is proceeded at T= -143 s by a small precursor, which could be shown via triangulation to originate from the position of SGR 1806-20.

INTEGRAL

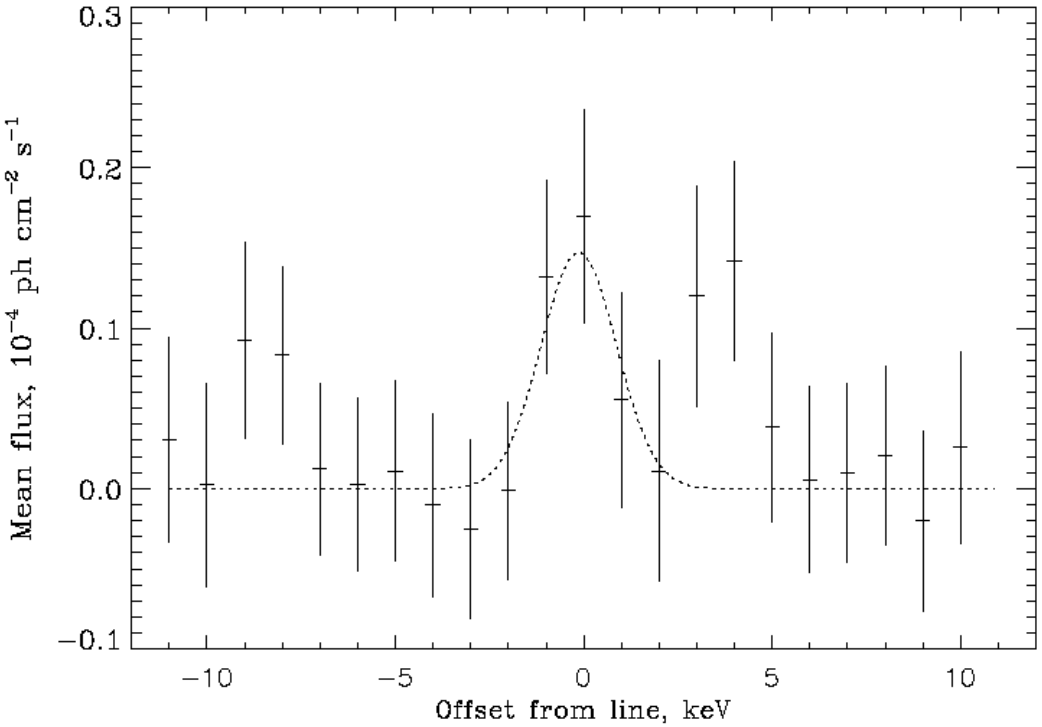

The SPI instrument on board INTEGRAL has observed the ^{60}Fe lines (at 1173 and 1333 keV) from the inner galaxy. The picture shows the combined ^{60}Fe signal from the two lines. The line flux is 3.7 ± 1.1 x 10^5 cm^{-2} s^{-1} per line.
The origin of the iron line is believed to be core-collapse supernovae which seed the interstellar medium with isotopes such as ^{60}Fe. From other SPI measurements of the ^{26}Al line the ratio ^{60}Fe/^{26}Al = 0.11 ±0.03 is derived, which is substantially smaller than predictions (0.40) for massive stars. This ratio supports the idea that there is an extra source of ^{26}Al in addition to the core-collapse supernovae.

INTEGRAL

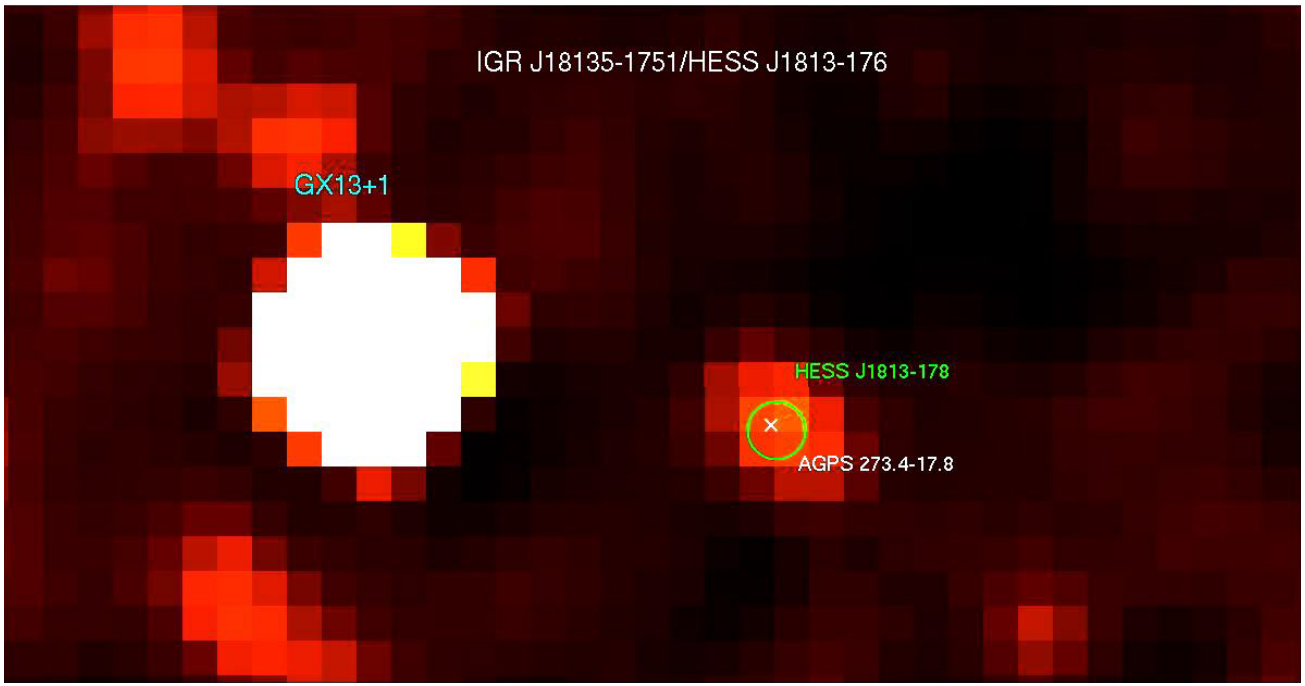

INTEGRAL has discovered, using the IBIS instrument, a new gamma-ray source (IGR J18135-1751). This source is remarkable, since it coincides spatially with one of the ten objects which have been seen during the first survey at TeV energies of the inner part of the galaxy: HESS J1813-178. This source is a powerful ultra-high energy emitter in the 0.2-10 TeV range. The X-ray counterpart (AGPS273.4-17.8) of the INTEGRAL source has an absorbed spectrum and is thought to be either a pulsar wind nebula or a supernova remnant. This picture shows the IBIS/ISGRI 20-100 keV image of IGR J18135-1751 as well as the position of HESS J1813-178 (green circle) and AGPS273.4-17.8 (white cross). The white spot on the left is the saturated image of the bright LMXB GX 13+1.

INTEGRAL

The central regions of our Galaxy, the Milky Way, as seen by INTEGRAL in gamma rays. With its superior ability to see faint details, INTEGRAL reveals the individual sources that comprised the foggy, soft gamma-ray background seen by previous observatories. The brightest 91 objects seen in this image were classified by INTEGRAL as individual sources, while the others appear too faint to be properly characterized at this stage.

INTEGRAL

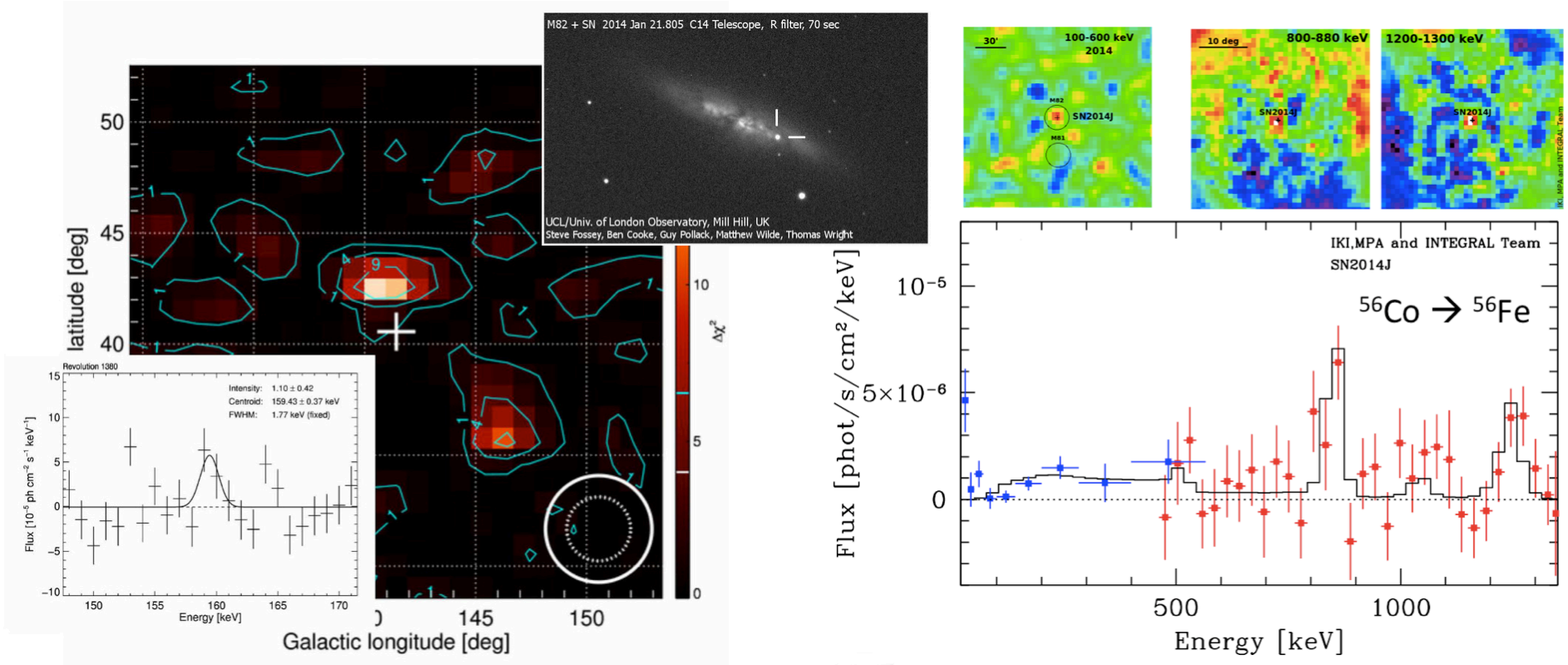

INTEGRAL for the first time, confirms by direct measurement of the primary gamma-ray lines the ^{56}Ni origins of SN light. The INTEGRAL measurements of this sufficiently-nearby SN provide a unique opportunity to compare the direct gamma-rays from the SN's energy source with the more-indirect other radiation. This will help astrophysicists to refine their models on how in fact these explosions do occur, because the explosion details affect how much new nuclei are created, and how they move and interact with the remainder of the exploding star. These observations constitute a reference in SNIa science, and thus an important scientific legacy for years to come.

INTEGRAL

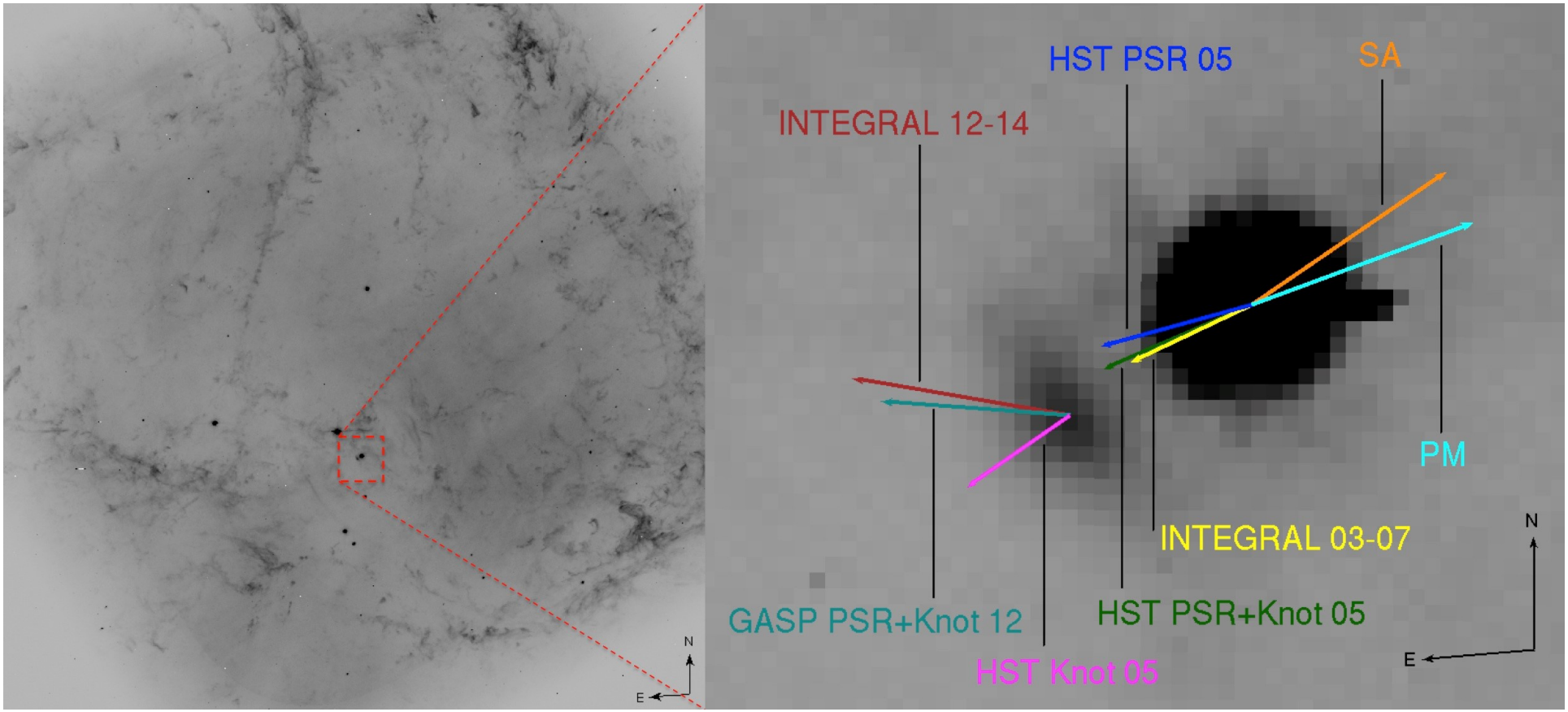

On the left, this HST image shows the inner part of the Crab nebula with the Crab pulsar and its near-by knot located 0.65" (1300 AU) south-east of the pulsar inside the red box. On the right, a zoomed view of the image is shown. The arrows indicate at different periods in time the polarization angle in the optical (HST in 2005 and GASP in 2012) and in hard X-rays (Integral in the period 2003-2007 and 2012-2014). Also indicated are the directions of the proper motion (PM) and spin axis (SA) of the pulsar.

INTEGRAL

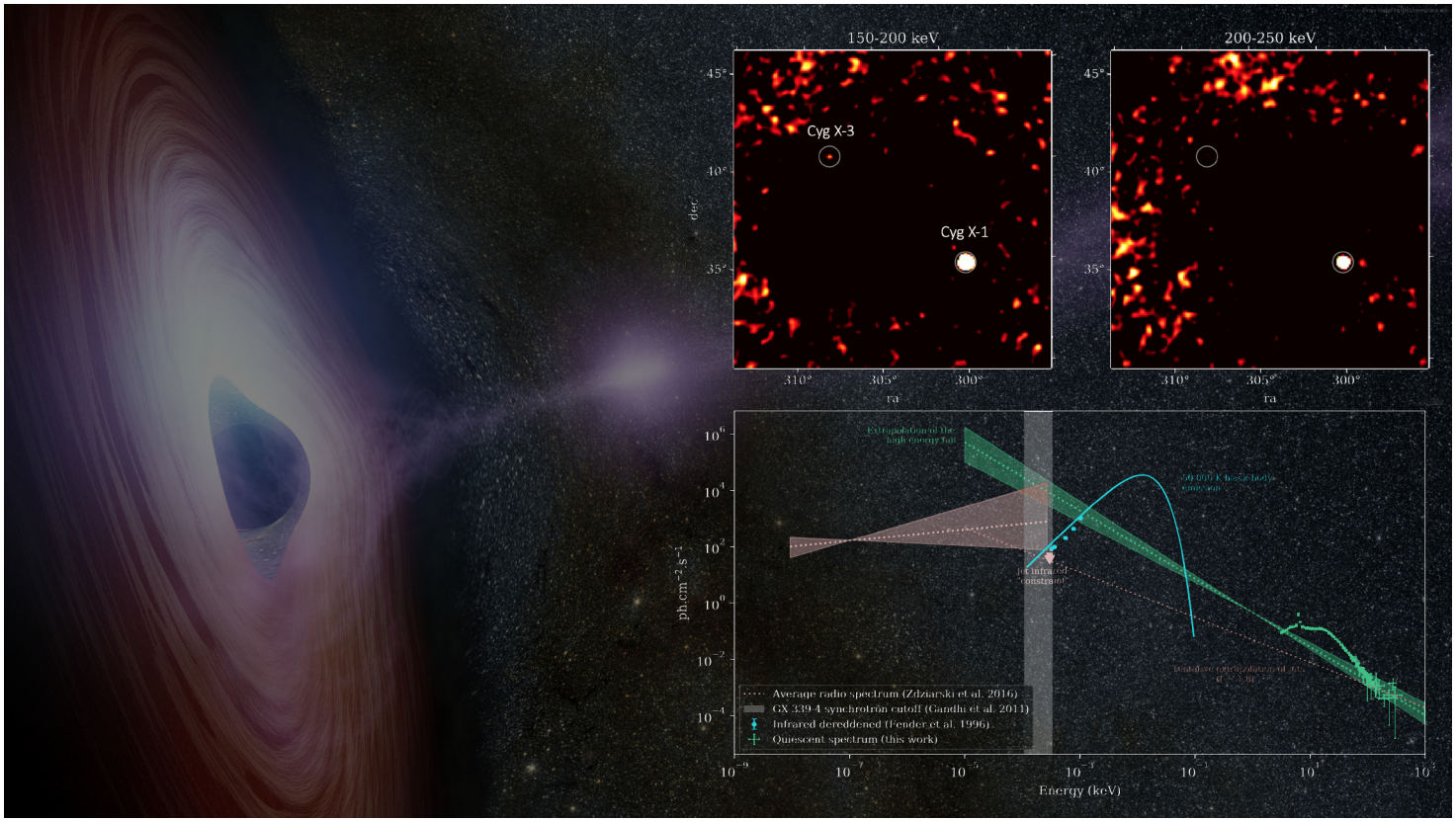

Cygnus X-3 is one of the first discovered X-ray binaries and the only bright compact binary system known to host a Wolf-Rayet star as a companion. The intense stellar wind created by this companion is one of the reasons why Cygnus X-3 exhibits a very peculiar spectral behavior. Indeed, it shows a wider variety of states than the two canonical ones usually observed in other standard X-ray binaries. Despite the fact that the source is well known since many years, very little is known about its spectral behavior beyond 50 keV. This lack of knowledge is especially due to the source being very faint at these energies. Thanks to INTEGRAL, it is possible to explore more than 16 years of observations, and so to probe the sky region of Cygnus X-3 with the best sensitivity ever. As shown at the top of the figure, one can detect the source up to 200 keV. Moreover, one can create six X-ray spectra from 3 to 200 keV, one for each observed spectral state of the source.

INTEGRAL

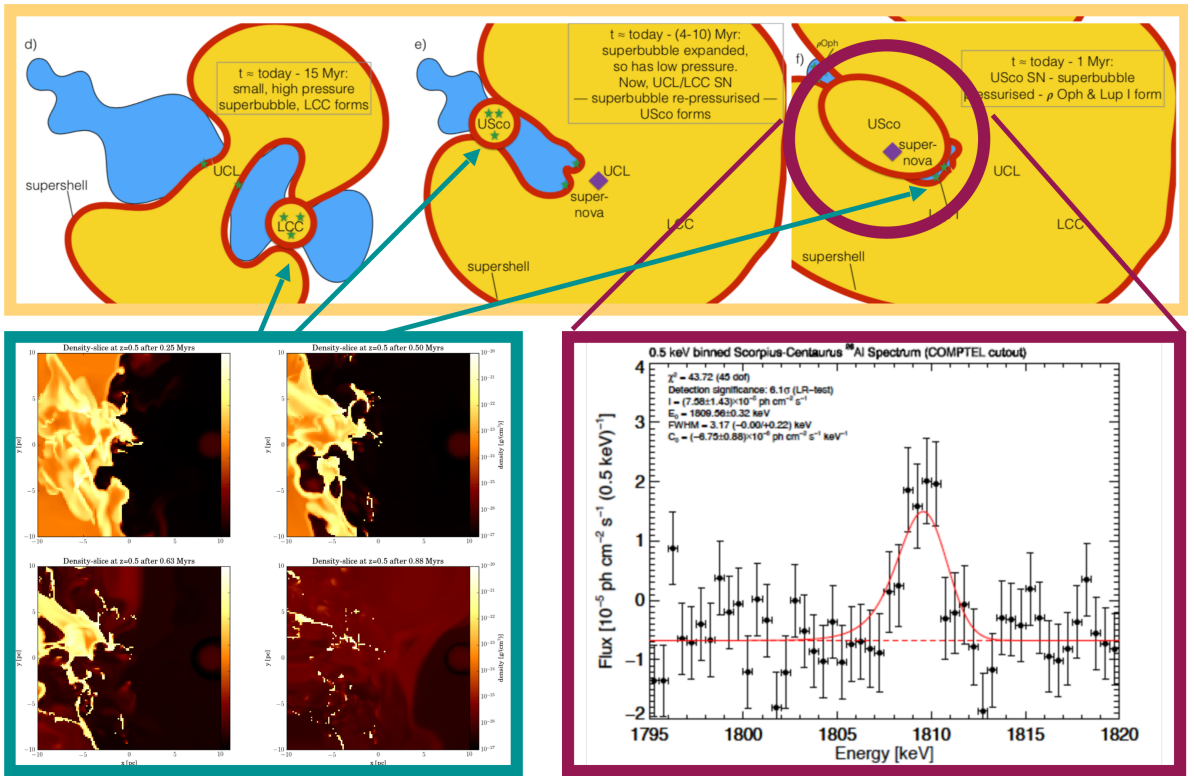

^{26}Al is uniquely produced by massive stars. These stars eject ^{26}Al through their winds and supernova explosions, which have a huge impact on the surrounding interstellar medium. Due to its short, in astronomical terms, decay time of a million years, ^{26}Al serves as evidence of very recent massive star activity. The detection of ^{26}Al towards the Scorpius-Centaurus region, therefore, provides a key piece of evidence in the reconstruction of the history of this massive star forming region.

Groups of stars first start to form in the densest part of a cloud, which in general may have a filamentary/elongated structure. The massive star activity forms a bubble of hot gas, which would be ^{26}Al enriched from massive-star ejecta. Gas may be compressed locally, leading to more star formation, but may also quickly escape along the minor axis of the cloud. In the tenuous medium around the cloud, the overpressured bubble could progress much more quickly than through the dense cloud, and thus reach and compress far-away regions of the cloud. The details of cloud compression and fragmentation of such a superbubble have been simulated and are shown in the bottom left part of the image. The ^{26}Al signal detected by INTEGRAL/SPI is independent proof for massive-star activity within approximately the last million years, and a key part of the study of how massive-star feedback works.

INTEGRAL

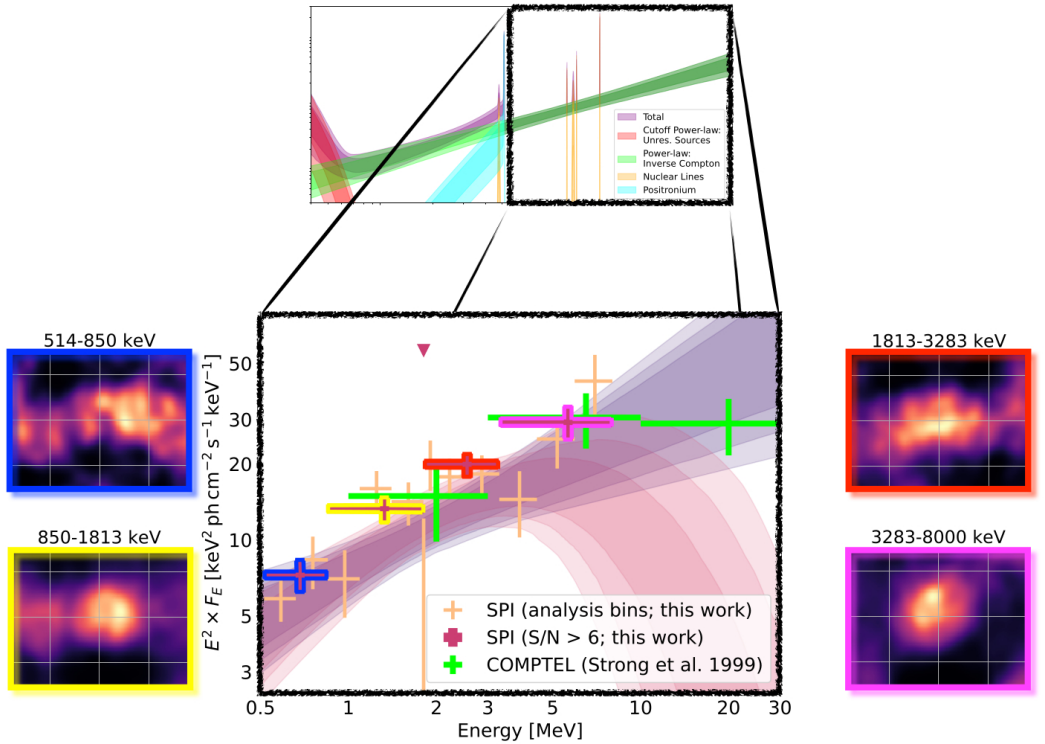

For more than 20 years, the Compton telescope, COMPTEL, onboard NASA's Compton Gamma-Ray Observatory, CGRO, set the standard for measurements of the extended emission of the Milky Way in the MeV range. This photon energy range harbours many emission mechanisms, for example, the annihilation of positrons in the interstellar medium, nuclear decays of radioactive isotopes, or the Inverse Compton scattering of electrons off the interstellar radiation field. These components are indicated in the top panel, showing the diffuse Galactic emission spectrum with its characteristic spectral features [1].

Cosmic-ray GeV electrons scatter off photons from star light in the optical and infrared (IR), as well as the cosmic microwave background (CMB). This scattering produces a smooth spectrum which peaks around 0.1 MeV for the CMB, around 0.5 MeV for IR, and potentially above 10 MeV for optical light. Together this makes the smooth spectrum shown in the zoomed-in panel [2]. Measuring the range between 0.5 MeV up to the limit of INTEGRAL/SPI at 8 MeV therefore constrains the transport properties of electrons as they scatter in IR and optical light.

With more than 16 years of data, SPI was able to set a new record in determining the diffuse emission spectrum in the 0.5-8.0 MeV band. The four coloured data points shown have a signal-to-noise ratio of 6 or more, superseding the data quality and precision of COMPTEL (green). The projections of the measured photons above the strong instrumental background [3] is shown for the four data points surrounding the bottom panel: there is clearly flux originating from the Galactic plane.

In this study, it was possible to test extreme assumptions on the propagation of GeV electrons: it appears that one common diffusion coefficient of 0.5 for the entire cosmic-ray electron spectrum best matches the INTEGRAL/SPI data. Another important finding in the work is that the absolute normalisation of most propagation models is a factor of 2-3 below the measurements, opening up the possibility of even more emission components such as unresolved point sources.

INTEGRAL

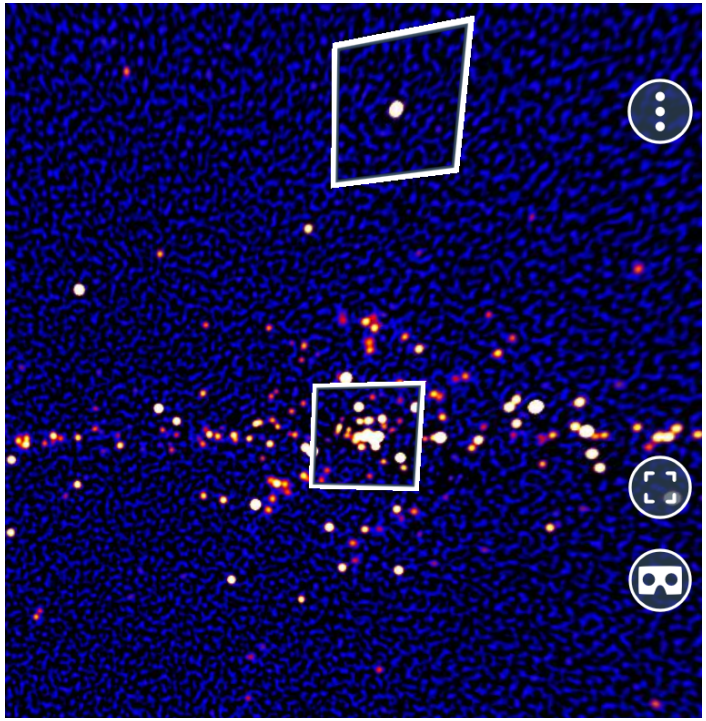

Thanks to the long-term operations of INTEGRAL, a large archive of unique observations of the hard X-ray sky has been accumulated. Taking advantage of the data gathered over 17 years with IBIS, a survey of hard X-ray sources in the 17-60 keV band has been conducted. The survey provides also flux information in different energy bands up to 290 keV. This new hard X-ray all-sky survey includes a number of deep extragalactic fields and the deepest ever hard X-ray survey of our Galaxy. The catalog of sources includes 929 objects detected on time-averaged sky map regions, i.e., mainly dominated by persistent hard X-ray emitters. Among the identified sources of known or suspected nature, 376 are associated with the Galaxy and Magellanic clouds, including 145 low-mass and 115 high-mass X-ray binaries, 79 cataclysmic variables, and 37 of other types. 440 are extragalactic, including 429 active galactic nuclei (AGNs), 2 ultra-luminous sources, one supernova (AT2018cow) and 8 galaxy clusters. 113 sources remain unclassified. 46 of these objects are detected in the hard X-ray band for the first time.

INTEGRAL

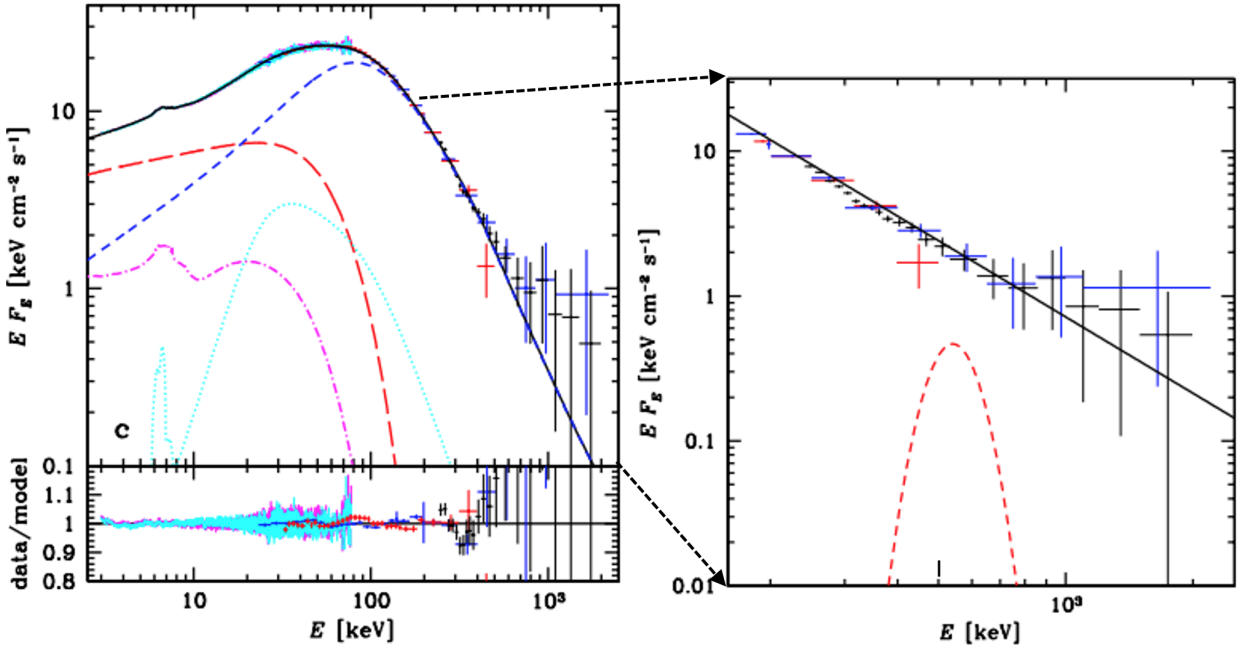

MAXI J1820+070 is a transient X-ray stellar binary, where matter outflowing from a low-mass donor star feeds a black hole. In March 2018, it had a spectacular outburst, during which it shined very bright X-rays and soft gamma-rays, observed by several satellite observatories, including INTEGRAL. The brightening lasted about half a year, during which the heated-up infalling gas shined several tens of thousand times stronger than the Sun.

A study based on INTEGRAL's main instruments, the spectrometer SPI and the imager IBIS, as well as the Nuclear Spectroscopic Telescope Array (NuSTAR) X-ray observatory focuses on modelling physical processes responsible for the observed high-energy photon energy distributions. During the initial rise of the outburst, the dominant physical process is Compton scattering, in which electrons moving with velocities comparable to the speed of light scatter some soft X-rays. In this process, the photon energy is amplified by a large factor, up to the hard X-ray and soft gamma-ray ranges. The electron distribution can be characterized by a temperature of a billion (109) Kelvin.

However, using INTEGRAL data, it appears that this distribution could no longer be described entirely by one temperature, since it showed a strong tail at high energies, consisting of electrons with energies many times the average thermal energy. The broad-band spectrum from Compton scattering is shown in the left panel of the image. The photons produced by the electron distribution tail were found to cross the threshold for production of electron-positron pairs, at 511 keV. Therefore, the presence of such pairs is expected, as well as their subsequent annihilation, which would give rise to a broadened line centred close to 511 keV. However, none was found, as shown in the right panel of the image. The maximum possible strength of such annihilation feature compatible with the data is shown by the red dashed curve. The consequence of this finding is that the size of the emitting plasma is relatively large, at least a few tens times the radius of the gravitational horizon of the black hole. This has important implications for theories of the mass flow onto black holes.

INTEGRAL

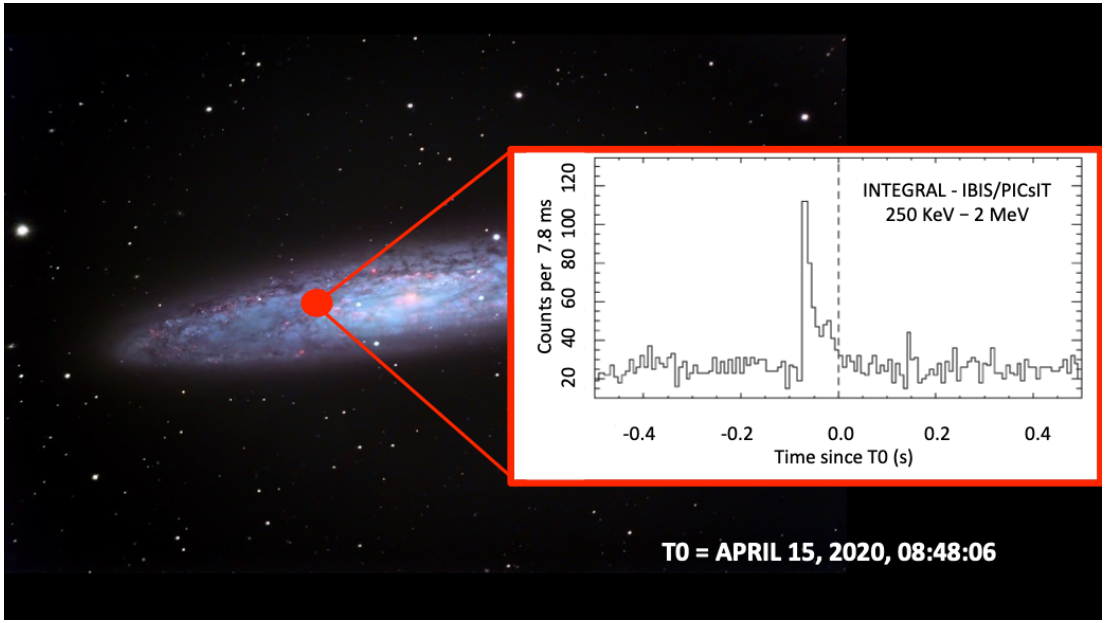

On 15 April 2020 a short and strong gamma-ray burst (GRB) was detected by several Gamma-ray satellites, featuring a fast rise time followed by an order of magnitude weaker tail. Shortly before 8:42 UT, GRB200415A triggered the Russian High-Energy Neutron Detector aboard NASA's Mars Odyssey satellite; about 400 sec later the burst triggered the Russian Konus instrument aboard NASA's Wind satellite. Finally, 4.5 sec later, the signal reached the Earth environment and triggered INTEGRAL's SPI and IBIS instruments, NASA's Fermi instruments and the Atmosphere-Space Interactions Monitor (ASIM) aboard the International Space Station (ISS). The light curve shown in the image is the burst as detected by the bottom layer of INTEGRAL/ISGRI, i.e., the PiCsIT instrument.

Taking advantage of the multiple detections from several spacecrafts orbiting in different parts of the Solar system, it was possible to locate the origin of the GRB emission within a narrow error box region: the radiation came from an extremely magnetized neutron star located in the neigh-boring galaxy NGC 253, know as the Sculptor galaxy. The background image shows an optical image of NGC 253, with a red dot indicating the origin of the burst.

This finding confirms that extremely powerful gamma-ray bursts are possibly generated by magnetars (neutron stars with extremely high magnetic fields of the order of 1014 to 1015 Gauss) in relatively close galaxies. During an active phase magnetars can emit random - milliseconds to several seconds long - hard-X-ray bursts, with peak luminosities of 1036 to 1043 erg per second, while giant flares, which are rare, emit at energies of about 1044 to 1046 erg. Such giant flares from other galaxies are detectable from instruments aboard satellites orbiting Earth or travelling in the Solar system.

A portion of the second-long initial pulse of a giant flare, similar to the one detected from the Sculptor galaxy, in some respect mimics short GRBs, which have recently been identified as the result from the merger of two neutron stars accompanied by gravitational-wave emission, i.e., GRB170817A and GW170817.

Galactic Sources

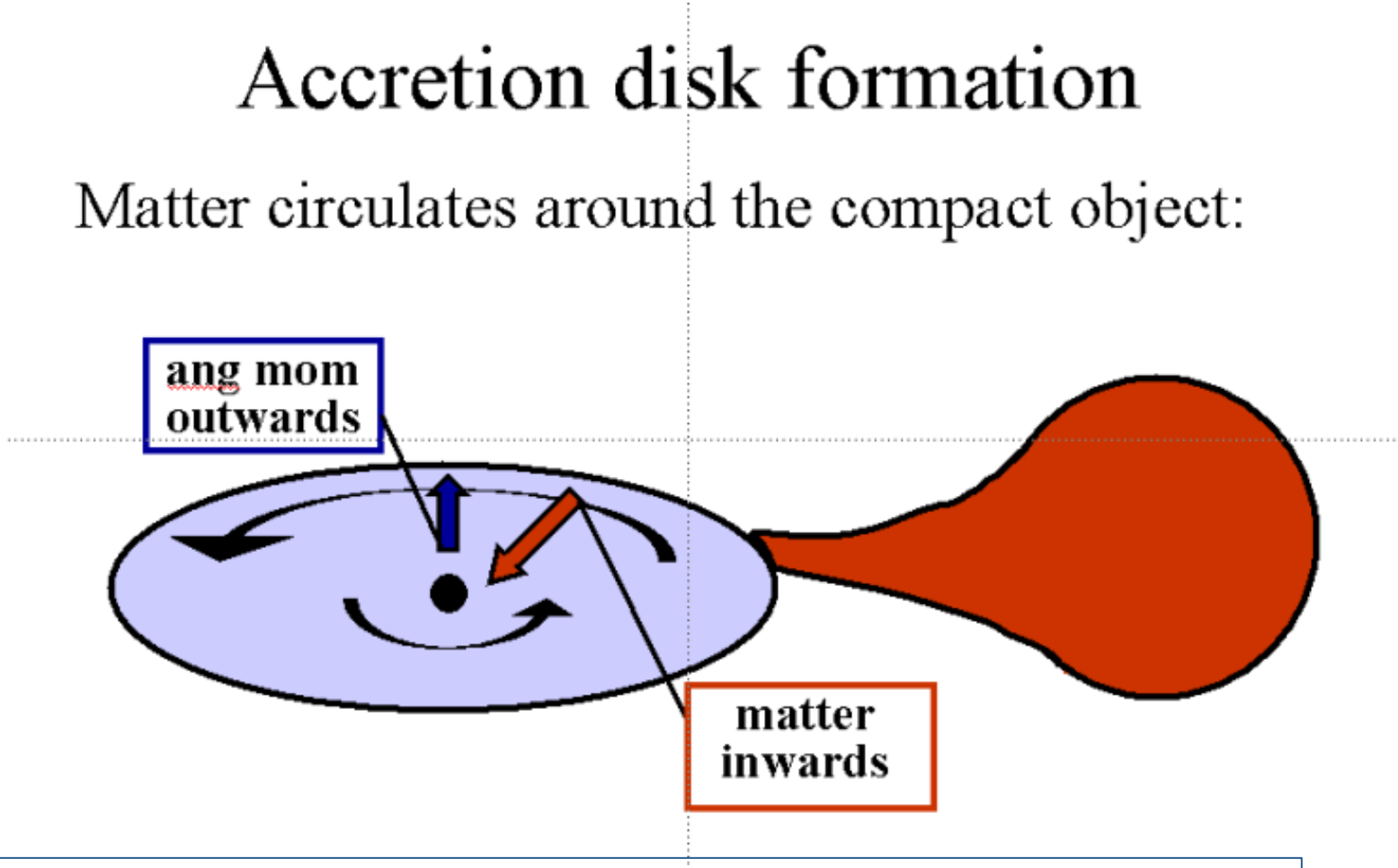

https://mssl.ucl.ac.uk/www_astro/lecturenotes/hea/hea.html

Galactic Sources

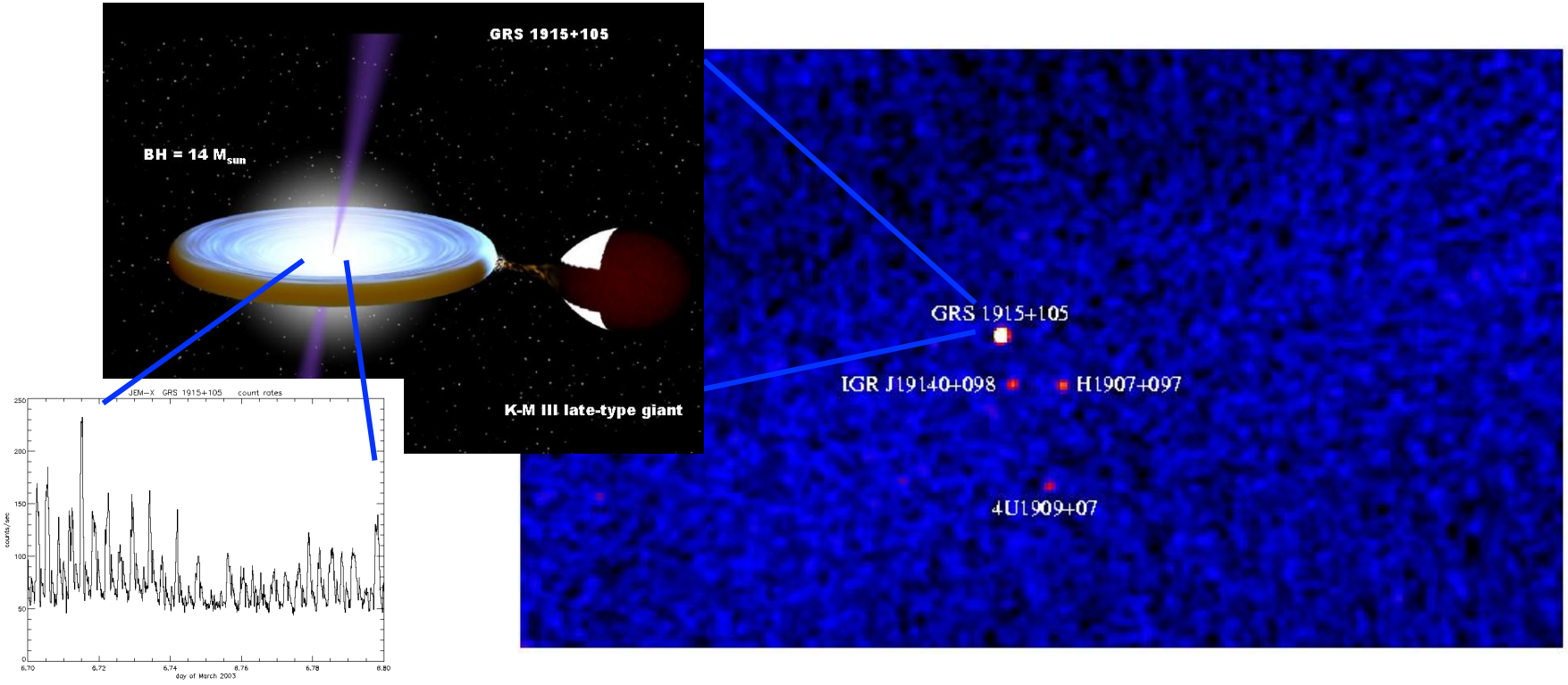

Galactic Sources

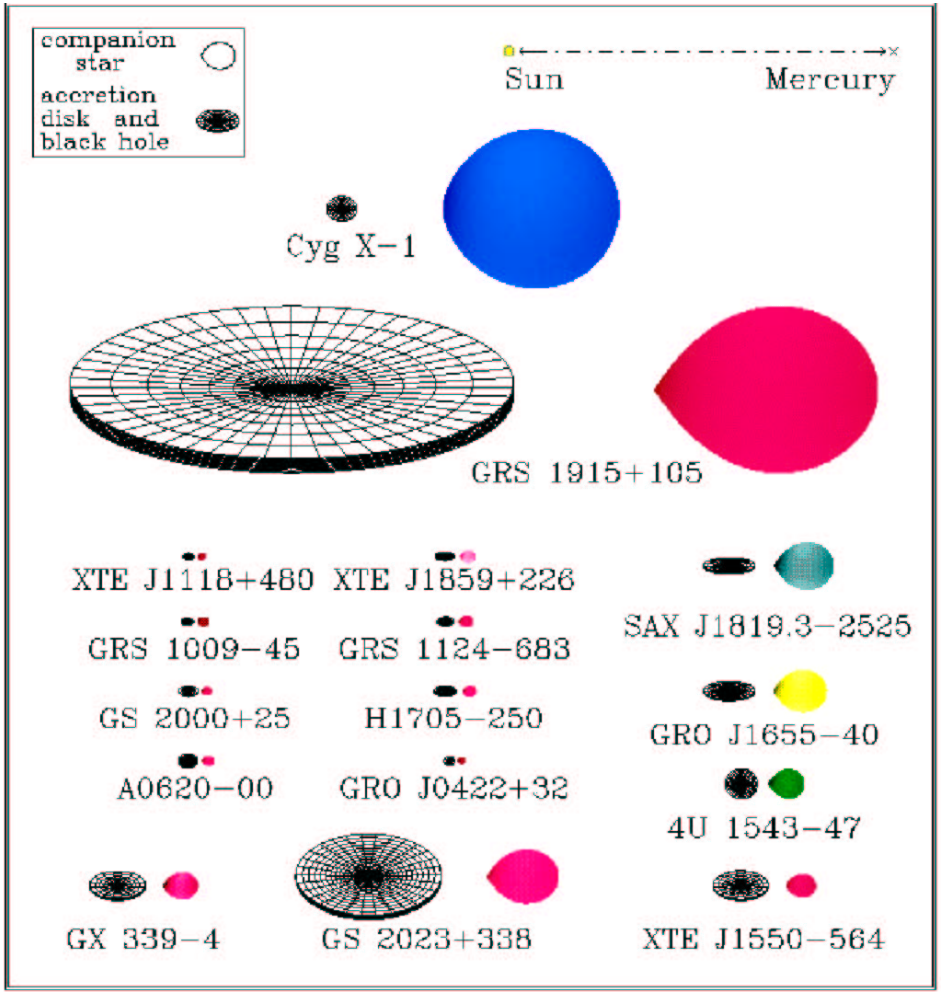

Credit: Jerome A. Orosz

Accretion Power

Accretion onto a compact object

- Principal mechanism for producing high-energy radiation
- Most efficient of energy production known in the Universe.

$$E_{acc} = G\frac{Mm}{R}$$

Gravitational potential energy released for body mass M and radius R when mass m accreted

Accretion Power

Example - neutron star

Accreting mass m=1kg onto a neutron star:

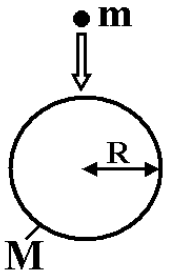

neutron star mass = 1 solar mass

R = 10 km

=> $\sim 10^{16}$ m Joules,

ie approx 10^{16} Joules per kg of accreted matter - as electromagnetic radiation

Efficiency of accretion

- Compare this to nuclear fusion
  H => He releases $\sim 0.007\ mc^2$
  $\sim 6 \times 10^{14}$ m Joules - **20x smaller** (for ns)

$$E_{acc} = G\frac{Mm}{R}$$

So energy released proportional to M/R ie the more compact a body is, the more efficient accretion will be.

Accretion Power

Origin of accreted matter

- Given M/R, luminosity produced depends on accretion rate, $\dot{m}$.

$$L_{acc} = \frac{dE_{acc}}{dt} = \frac{GM}{R}\frac{dm}{dt} = \frac{GM\dot{m}}{R}$$

- Where does accreted matter come from? ISM? No - too small. Companion? Yes.

Accretion Power

The Eddington Luminosity

- There is a limit to which luminosity can be produced by a given object, known as the Eddington luminosity.

- Effectively this is when the inward gravitational force on matter is balanced by the outward transfer of momentum by radiation.

Accretion Power

Eddington Luminosity

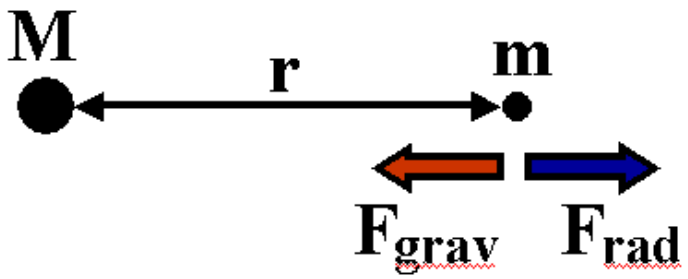

Accretion rate controlled by momentum transferred from radiation to mass

$$F_{grav} = G\frac{Mm}{r^2} Newton$$

Note that R is now negligible wrt r

Outgoing photons from M scatter material (electrons and protons) accreting.

Accretion Power

Scattering

L = accretion luminosity

no. photons crossing at r per second $= \frac{L}{4\pi r^2}\frac{1}{h\nu}$ photons m^{-2} s^{-1}

Scattering cross-section will be Thomson cross-section σ_e; so no. scatterings per sec:

$$\frac{L\sigma_e}{4\pi r^2 h\upsilon}$$

Accretion Power

Momentum transferred from photon to particle:

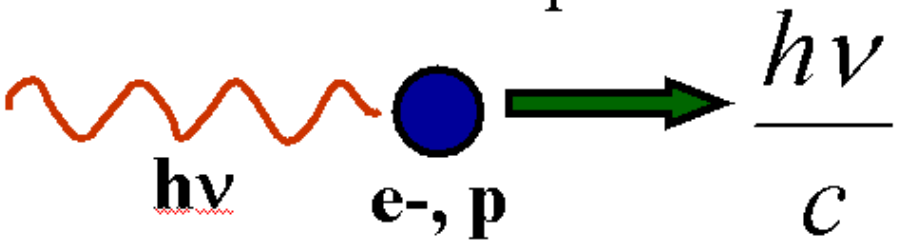

Momentum gained by particle per second = force exerted by photons on particles

$$\frac{L\sigma_e}{4\pi r^2 h\upsilon}\frac{h\nu}{c} = \frac{L\sigma_e}{4\pi r^2 c} Newton$$

Accretion Power

Eddington Limit

radiation pressure = gravitational pull

At this point accretion stops, effectively imposing a 'limit' on the luminosity of a given body. $\frac{L\sigma_e}{4\pi r^2 c} = G\frac{Mm}{r^2}$

So the Eddington luminosity is: $L = \frac{4\pi cGMm}{\sigma_e}$

Accretion Power

Assumptions made

- **Accretion flow steady + spherically symmetric:** eg. in supernovae, L_{Edd} exceeded by many orders of magnitude.

- **Material fully ionized and mostly hydrogen**: heavies cause problems and may reduce ionized fraction - but OK for X-ray sources

Accretion Power

Accretion modes in binaries

ie. binary systems which contain a compact star, either white dwarf, neutron star or black hole.

(1) Roche Lobe overflow

(2) Stellar wind

- correspond to different types of X-ray binaries

Accretion

Roche Lobe Overflow

- Compact star M_1 and normal star M_2

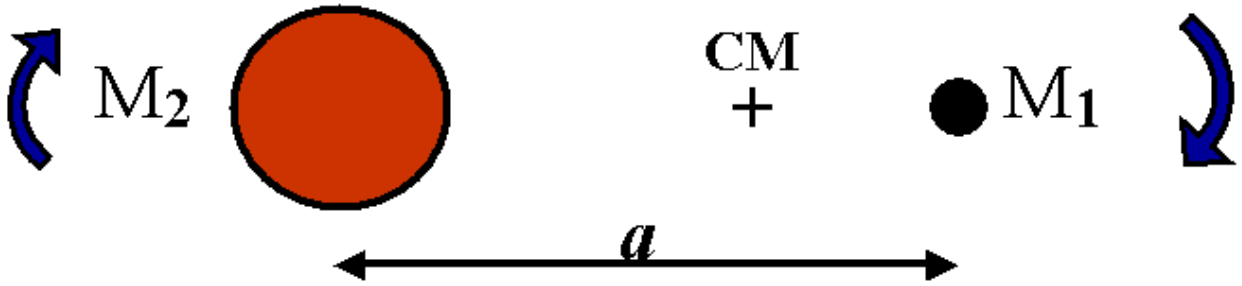

- normal star expanded or binary separation decreased => normal star feeds compact

Accretion

Matter circulates around the compact object:

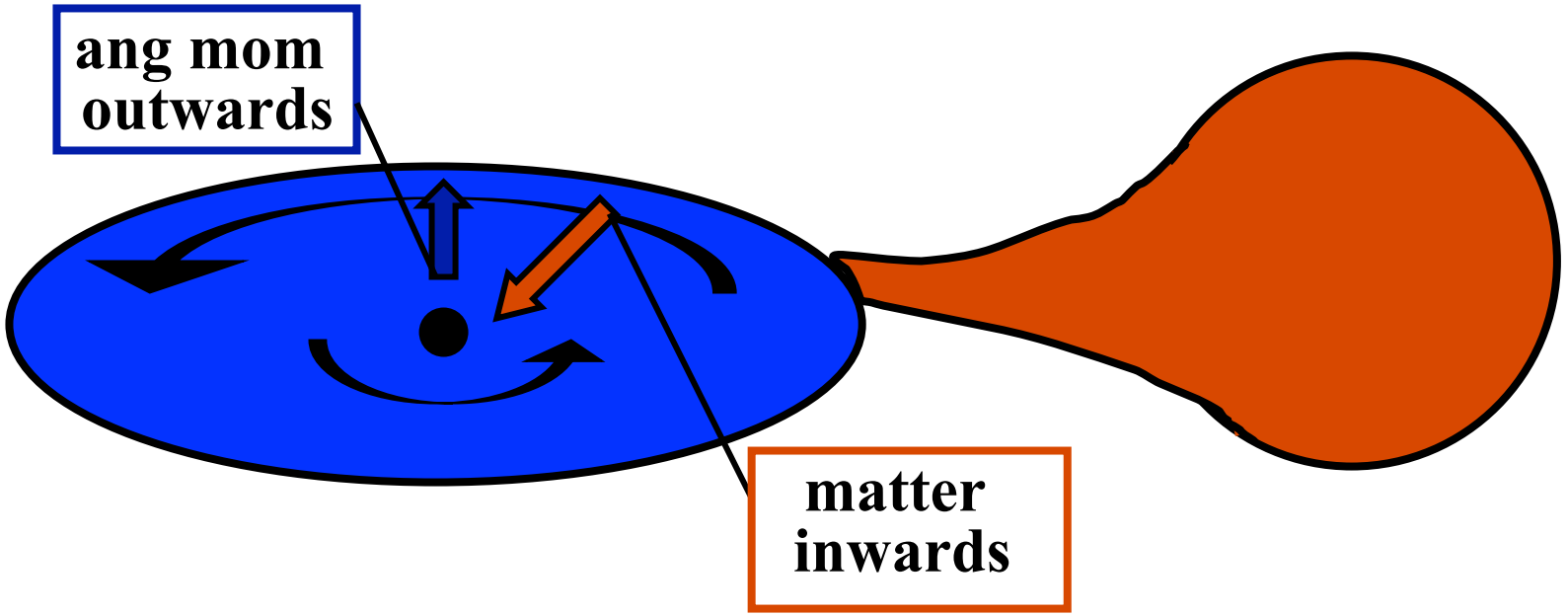

Accretion

Energy losses from the disk

$E_{bind} = \frac{GMm}{2R}$ and $L_{bind} = \frac{GM\dot{M}}{2R}$

$E_{bind} \sim 0$

So the energy which has been lost in the disk by m is:

$E_{disk} = \frac{GMm}{2R}$

and $L_{disk} = \frac{GM\dot{M}}{2R}$

$= \frac{1}{2}L_{acc}$

Disk structure

Half of the accretion luminosity is released very close to the star.

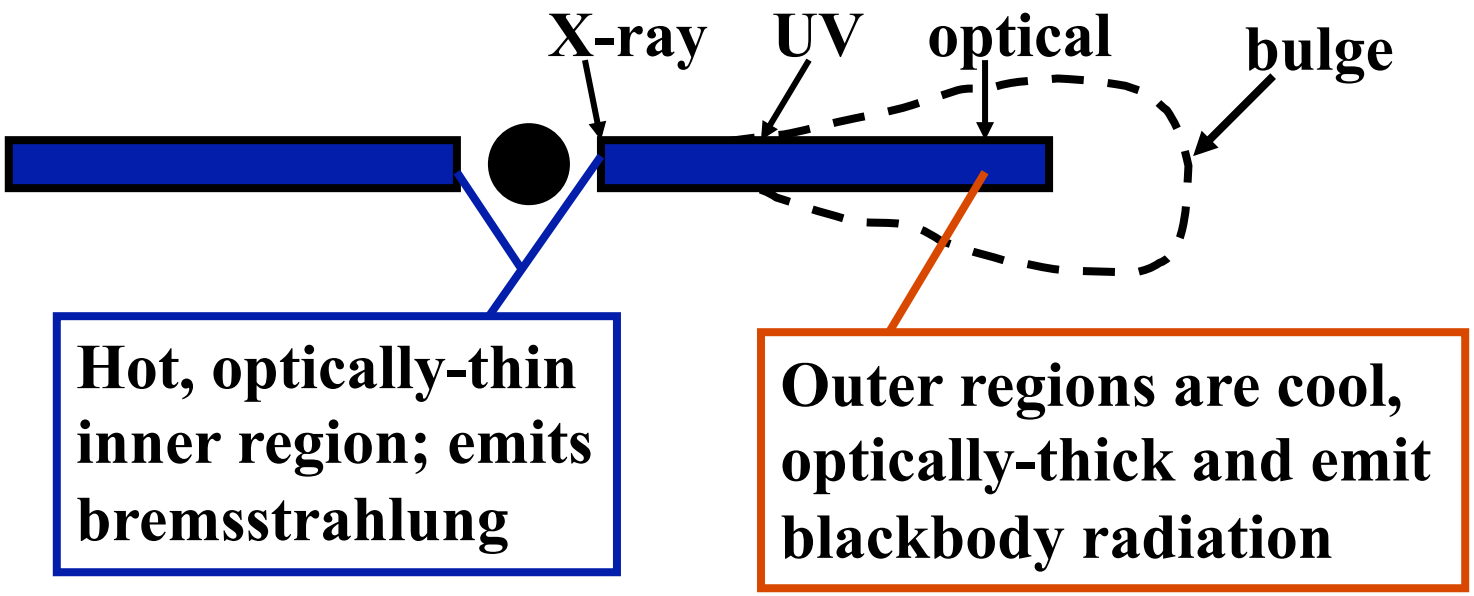

Stellar Wind Accretion

Stellar Wind Model

Early-type stars have intense and highly supersonic winds. Mass loss rates - 10^{-6} to 10^{-5} solar masses per year.

For compact star - early star binary, compact star accretes if

$$\frac{GMm}{r} > \frac{1}{2} m(v_w^2 + v_{ns}^2)$$

Stellar Wind Accretion

Thus :

$$r_{acc} = \frac{2GM}{v_w^2 + v_{ns}^2}$$

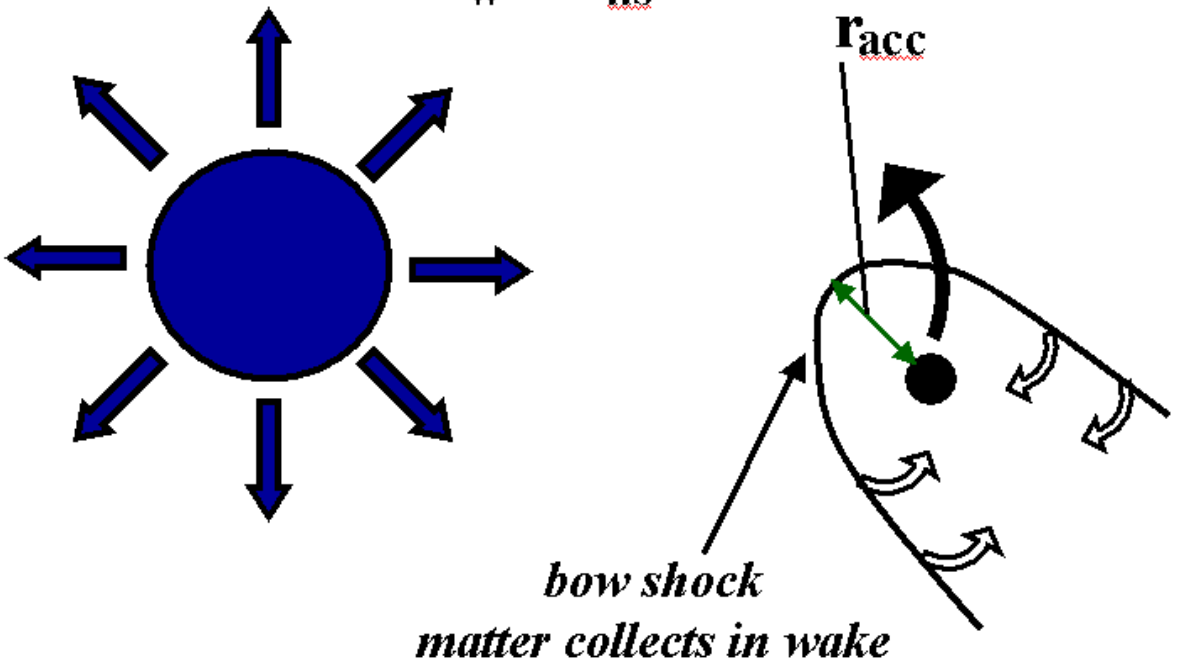

Accretion

Types of X-ray Binaries

Group I	**Group II**
Luminous (early, massive opt countpart) *(high-mass systems)*	Optically faint (blue) opt counterpart *(low-mass systems)*
hard X-ray spectra *(T>100 million K)*	soft X-ray spectra *(T~30-80 million K)*
often pulsating *X-ray eclipses*	non-pulsating *no X-ray eclipses*
Galactic plane *Population I*	Gal. Centre + bulge *older, population II*

The Compton Gamma Ray Observatory

http://cossc.gsfc.nasa.gov

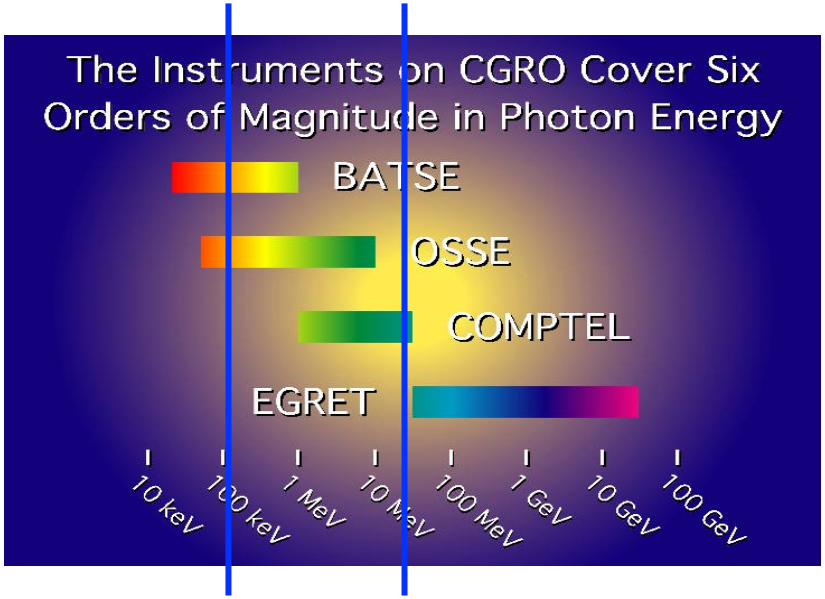

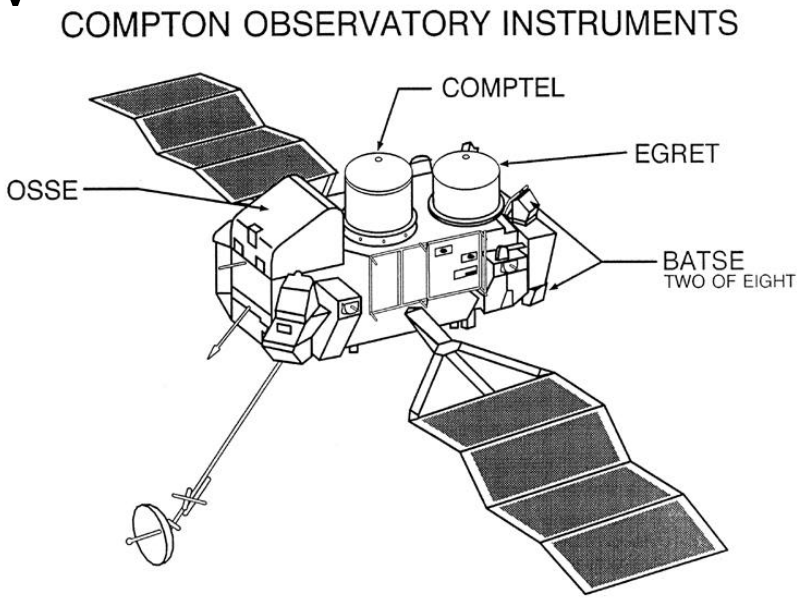

The Compton Gamma Ray Observatory (CGRO) is a sophisticated satellite observatory dedicated to observing the high-energy Universe. It is the second in NASA's program of orbiting "Great Observatories", following the Hubble Space Telescope.
While Hubble's instruments operate at visible and ultraviolet wavelengths, Compton carries a collection of four instruments which together can detect an unprecedented broad range of high-energy radiation called gamma rays. These instruments are the Burst And Transient Source Experiment (BATSE), the Oriented Scintillation Spectrometer Experiment (OSSE), the Imaging Compton Telescope (COMPTEL), and the Energetic Gamma Ray Experiment Telescope (EGRET).

The Compton Gamma Ray Observatory

Table 1: SUMMARY OF *COMPTON* GRO DETECTOR CHARACTERISTICS

	OSSE	COMPTEL	EGRET	BATSE	
				LARGE AREA	SPECTROSCOPY
ENERGY RANGE (MeV)	0.05 to 10.0	0.8 to 30.0	20 to 3 x 10^4	0.03 to 1.9	0.015 to 110
ENERGY RESOLUTION (FWHM)	12.5% at 0.2 MeV 6.8% at 1.0 MeV 4.0% at 5.0 MeV	8.8% at 1.27 MeV 6.5% at 2.75 MeV 6.3% at 4.43 MeV	~20% 100 to 2000 MeV	32% at 0.06 MeV 27% at 0.09 MeV 20% at 0.66 MeV	0.2% at 0.09 MeV 7.2% at 0.66 MeV 5.8% at 1.17 MeV
EFFECTIVE AREA (cm^2)	2013 at 0.2 MeV 1480 at 1.0 MeV 569 at 5.0 MeV	25.8 at 1.27 MeV 29.3 at 2.75 MeV 29.4 at 4.43 MeV	1200 at 100 MeV 1600 at 500 MeV 1400 at 3000 MeV	1000 eq. at 0.03 MeV 1800 eq. at 0.1 MeV 550 eq. at 0.66 MeV	100 eq. at 0.3 MeV 127 eq. at 0.2 MeV 52 eq. at 3 MeV
POSITION LOCALIZATION (STRONG SOURCE)	10 arc min square error box (special mode; 0.1 x Crab spectrum)	0.5 - 1.0 deg (90% confidence 0.2 x Crab spectrum)	5 to 10 arc min (1σ radius; 0.2 x Crab spectrum)	3° (strong burst)	———
FIELD OF VIEW	3.8° x 11.4°	~ 64°	~ 0.6 sr	4 π sr	4 π sr
MAXIMUM EFFECTIVE GEOMETRIC FACTOR (cm^2 sr)	13	30	1050 (~ 500 MeV)	15000	5000
ESTIMATED SOURCE SENSITIVITY (5×10^6 sec; on source, off Galactic Plane) LINE	(3-8) x 10^{-5} cm^{-2} s^{-1}	1.5 x 10^{-5} to 6 x 10^{-5} cm^{-2} s^{-1}			0.4% equivalent width (5 sec integration)
CONTINUUM	3 x 10^{-7} cm^{-2} s^{-1} keV^{-1} (@1 MeV)	1.6 x 10^{-4} cm^{-2} s^{-1} (3 σ detection, 1-30 MeV)	7 x 10^{-8} cm^{-2} s^{-1} (> 100 MeV) 2 x 10^{-8} cm^{-2} s^{-1} (> 1000 MeV)	3 x 10^{-8} erg cm^{-2} (1 sec-burst)	

CGRO performance

	BATSE	OSSE	COMPTEL	EGRET
Developer	NASA/Marshall	Naval Research Lab	Univ. N.H. & MPE	NASA/Goddard
Energy Range (MeV)	0.03 to 1.9	0.05 to 10.0	0.08 to 30.0	30.0 to 30000.0
Field of View	entire sky	3.0 x 11.4 degrees	64 degrees	0.6 steradians
Spectral Resolution (FWHM)	32 % at 0.06 MeV 27 % at 0.09 MeV 20 % at 0.66 MeV	12.5 % at 0.2 MeV 5. % at 1.0 MeV 4.0 % at 5.0 MeV	8.8 % at 1.27 MeV 6.5 % at 2.75 MeV 6.3 % at 4.43 MeV	20 %
Effective Area (cm^2)	1000 ea. at 0.03 MeV 1800 ea. at 0.1 MeV 550 ea. at 0.55 MeV	2013 at 0.2 MeV 1400 at 1.0 MeV 55 at 5.0 MeV	25.0 at 1.27 MeV 29.3 at 2.75 MeV 29.4 at 4.43 MeV	1200 at 100 Mev 1600 at 500 MeV 1400 at 3000 MeV
Spatial Resolution (for strong sources)	3 degrees	10 x 10 arcminutes	0.5 - 1.0 degrees	5 - 10 arcminutes

The Compton Gamma Ray Observatory

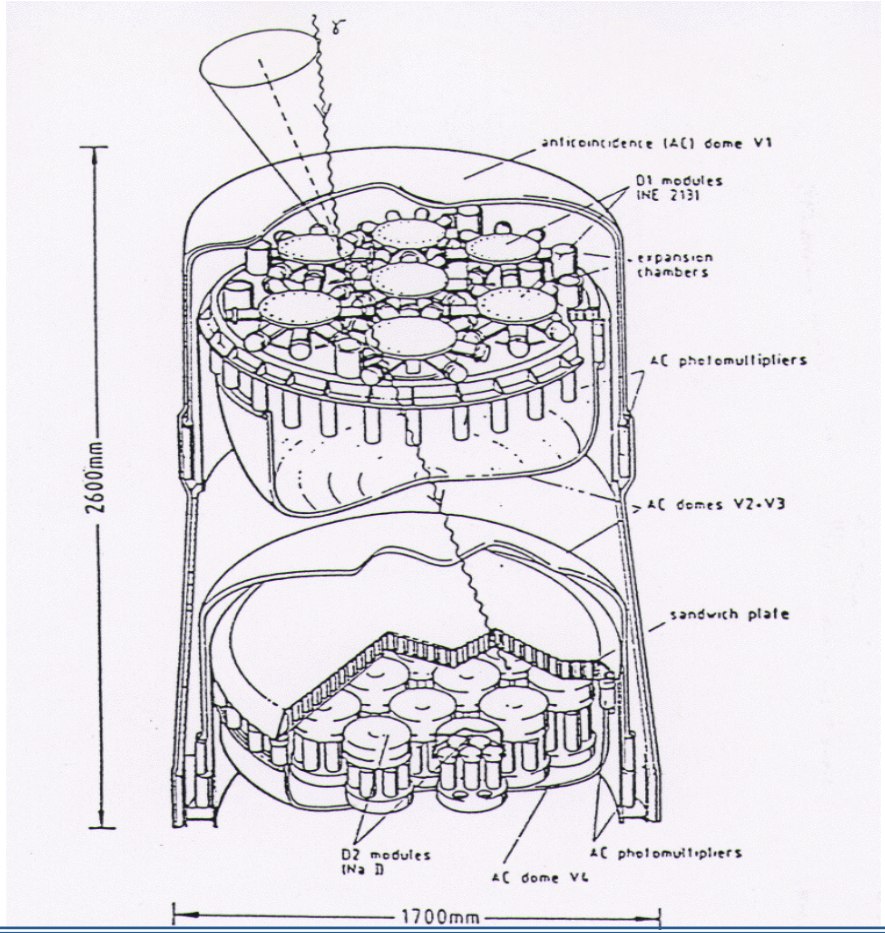

COMPTEL

- 0.05-30 MeV
- Radioactive elements map, pulsars, a flaring black hole candidates, blazars, solar flares

Telescopi Compton

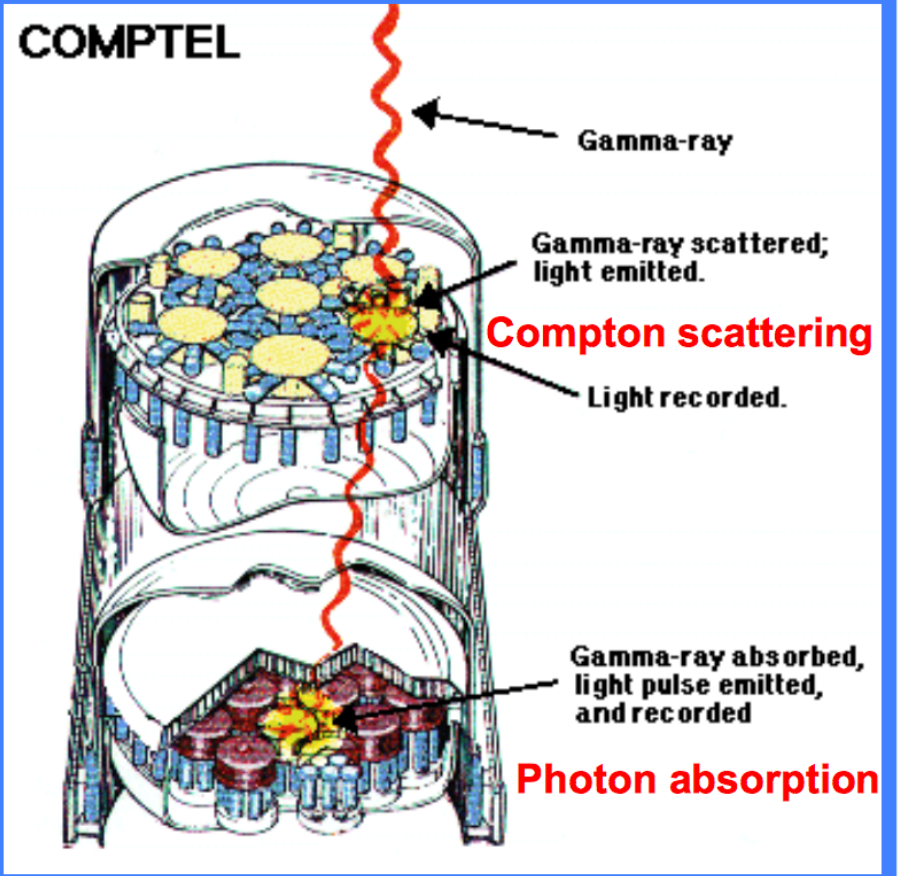

Two-level instruments:
1st level: the γ-ray Compton scatters off an electron in a **liquid scintillator**. The scattered photon enters into a **2nd level scintillator** (NaI) and is absorbed. Phototubes can determine the interaction points at the two layers and record the amount of energy deposited in each layer.

It is possible to reconstruct the angle of incidence the photon made wrt the original direction using the Compton scattering law, linking this angle and the energy of the scattered photon
(2nd level) and the scattering electron (1st level).

"Event circle" (ring on the sky), poor angular resolution (but multiple photons can help to reconstruct the position)

Compton Imaging

COMPTEL on CGRO

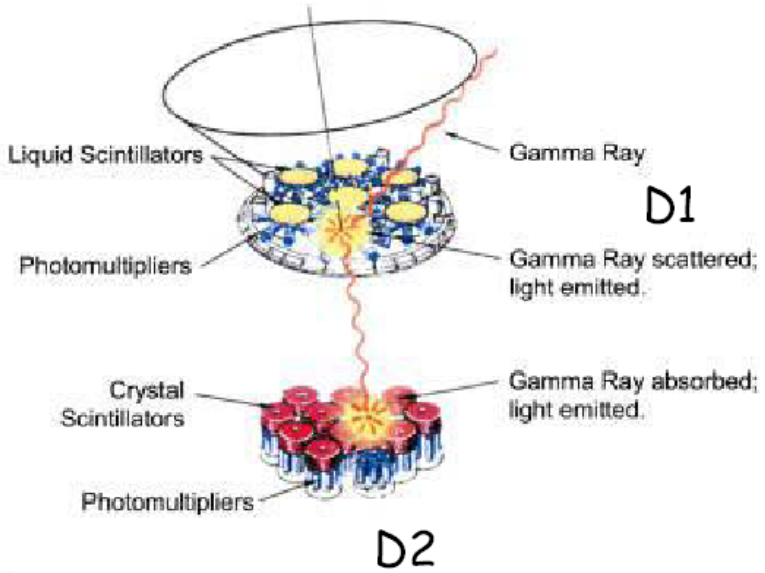

Compton Imaging

Detection of Gamma Radiation

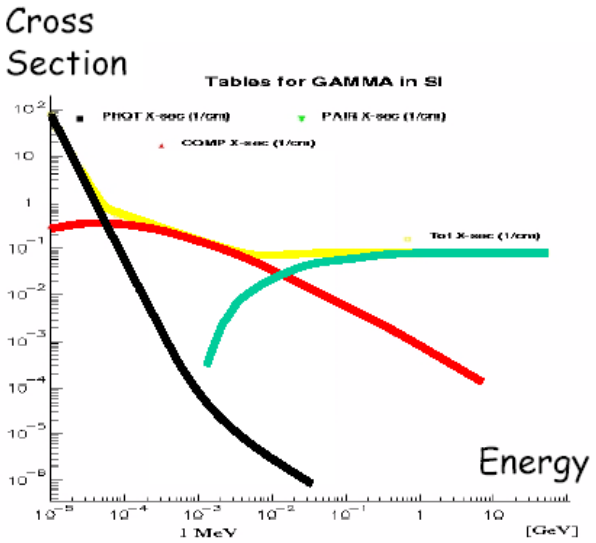

Photoeffect(< 100 keV)

Photons effectively blocked and stopped

Telescopes:

Collimators
Coded Mask Systems

Compton Scattering (0.2-10 MeV)
Photon Crossection Minimum
Scattered photons with long range
Telescope:
Compton Camera Coincidence System

Pair Creation (> 10 MeV)
Photons completely converted to e^+e^-

Telescope:
Tracking chambers to visualize the pairs

Sensitivity

G. Kanbach et al. / New Astronomy Reviews 48 (2004) 275–280

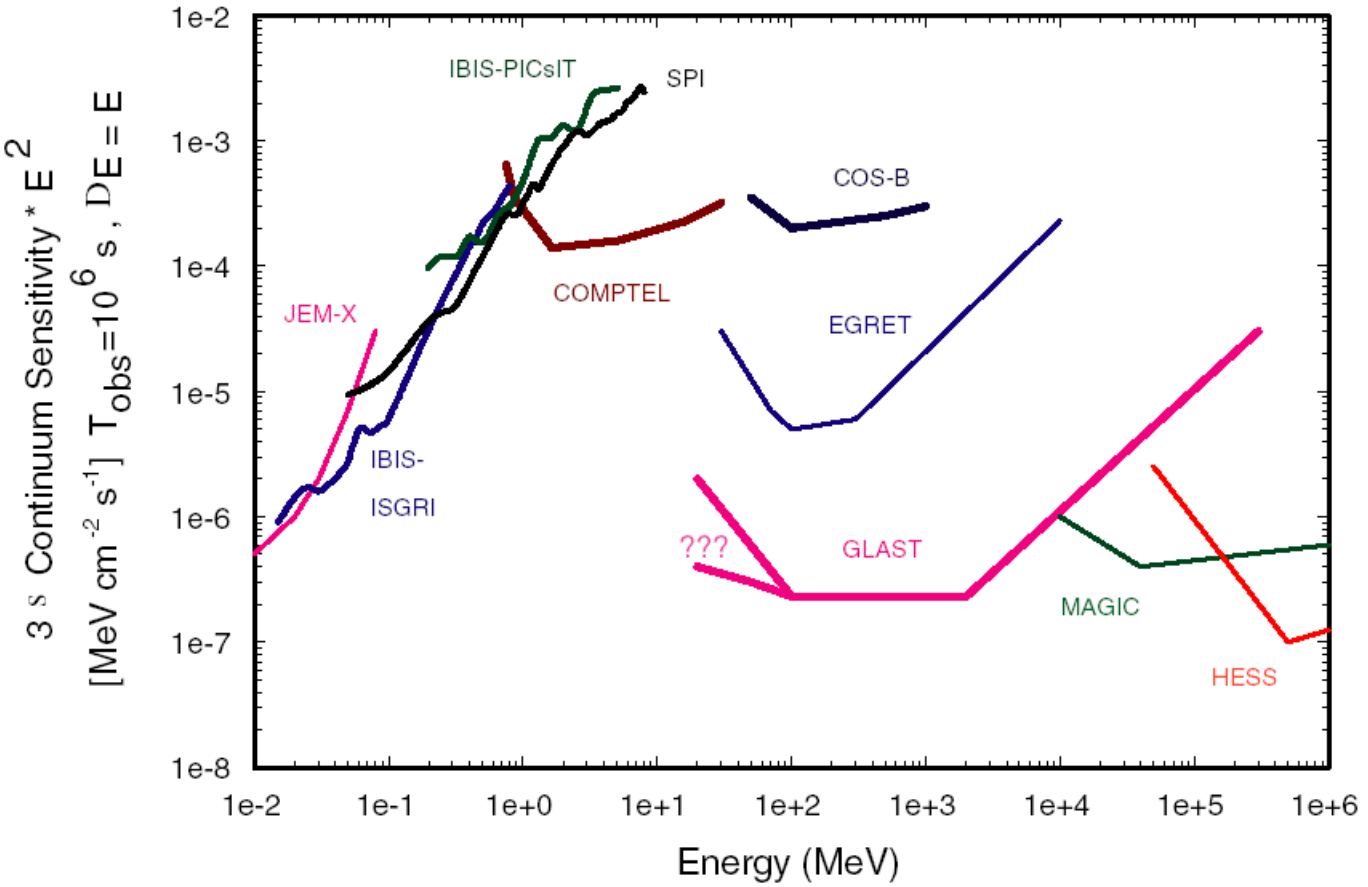

Compton Imaging

Low to Medium Energy Gamma-Ray Astronomy

or

what is the promise and hope for astrophysics in the energy range

" few 100 keV to ~ 50 MeV "

???

Compton Imaging

Kinematics
(target at rest)

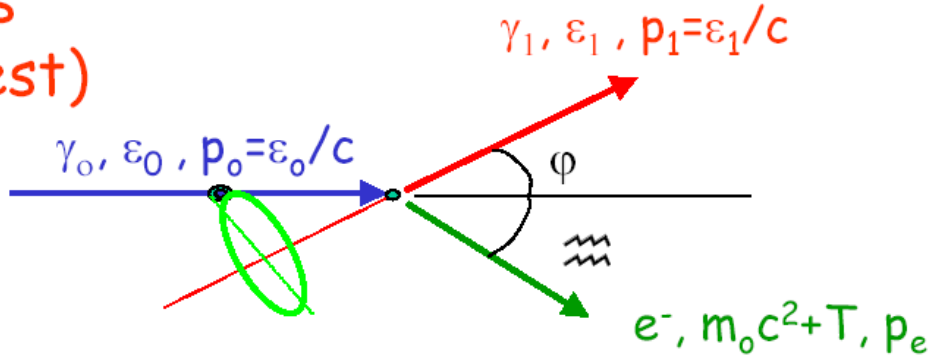

Energy: $\varepsilon_0 = \varepsilon_1 + T$

Momentum:

$$\varepsilon_0 = \varepsilon_1 \cos\varphi + pc\cos\vartheta$$

$$\varepsilon_1 \sin\varphi = pc\sin\vartheta$$

where $pc = \sqrt{T(T+2m_0c^2)}$

Compton Equation:

$$\cos\varphi = 1 - m_0c^2\left(\frac{1}{\varepsilon_1} - \frac{1}{\varepsilon_0}\right)$$

Compton Imaging

The ‚classical' Compton telescope

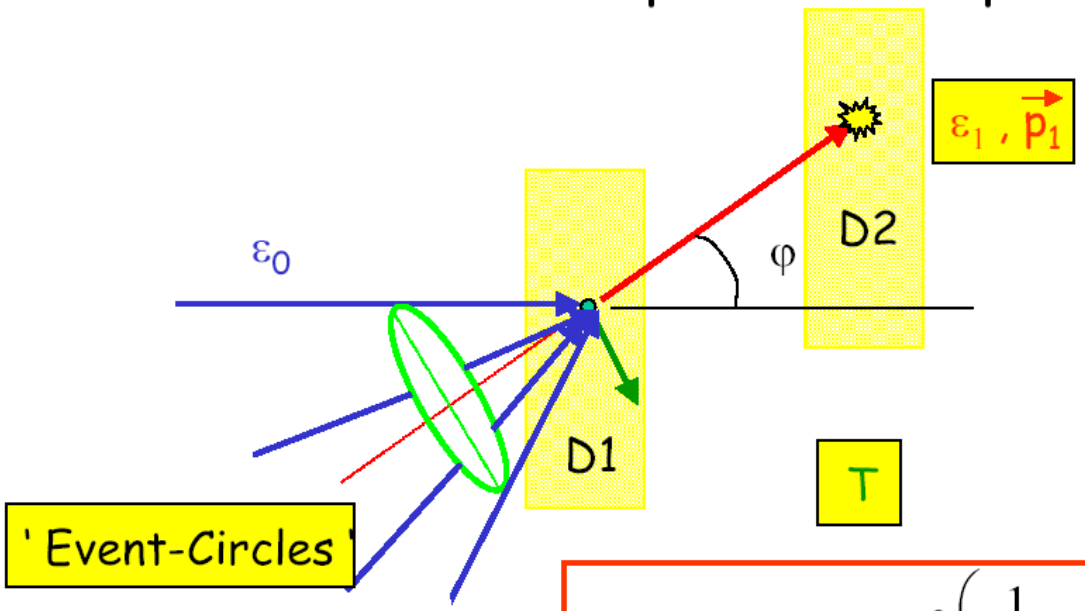

$$\cos\varphi = 1 - m_0 c^2 \left(\frac{1}{\varepsilon_1} - \frac{1}{\varepsilon_0} \right)$$

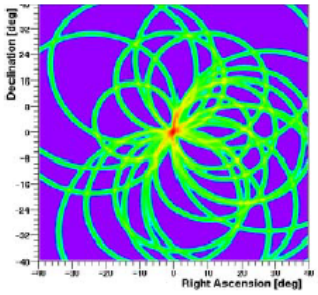

Compton Imaging

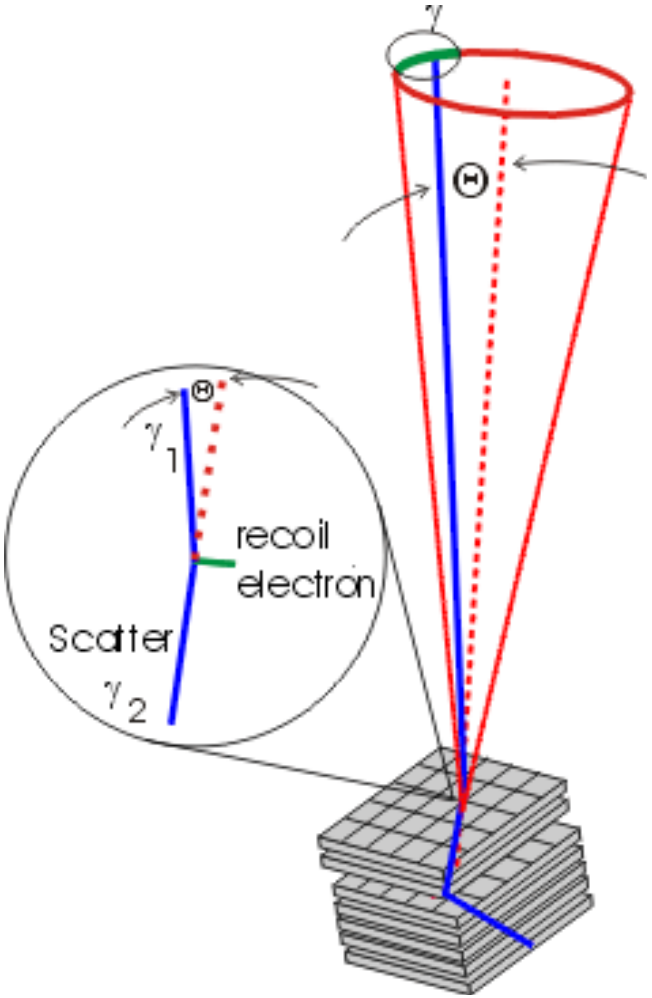

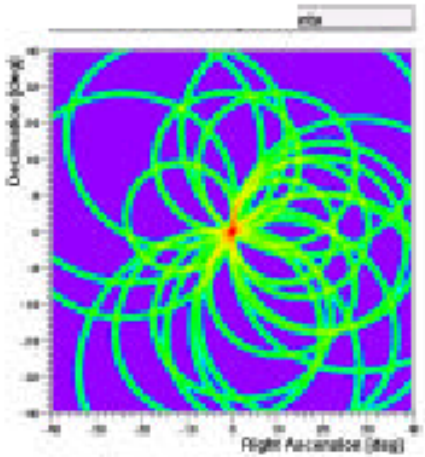

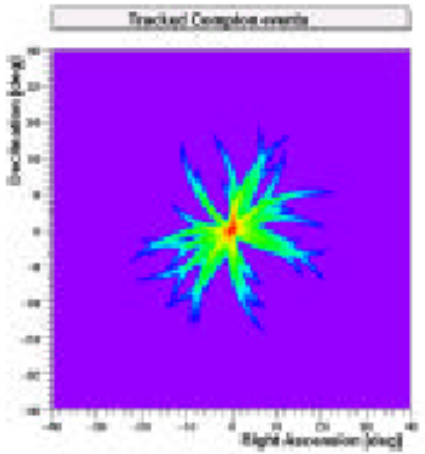

Compton Imaging

Coincidence Detector Schematics

Classical Compton Event Circles (no electron tracking)	Reduced Compton circles of events with electron track	Direct imaging of pair-creation events

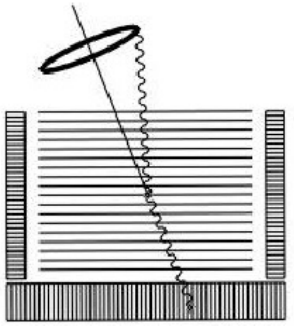

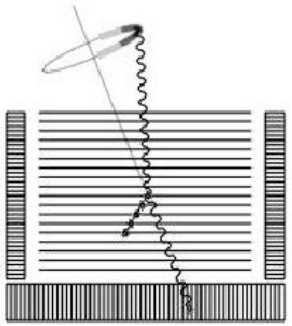

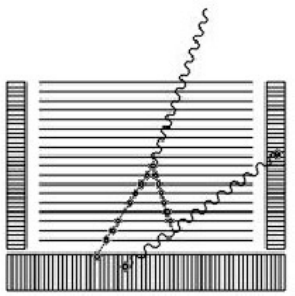

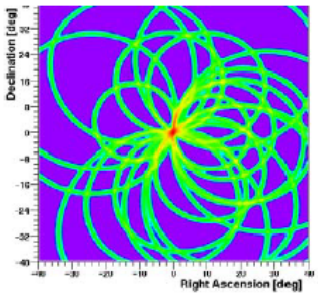

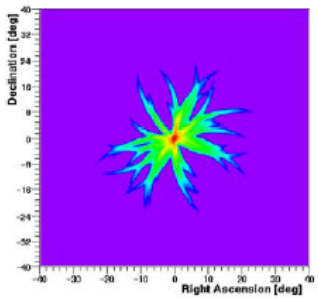

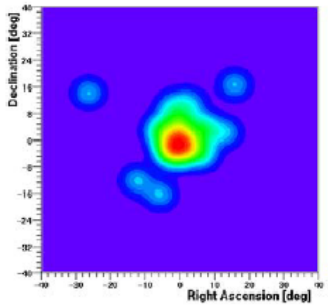

Compton Imaging

Sensitivities

Generations of γ-ray Missions:

1. COMPTEL ⇔ COS-B
2. MEGA (~2006) ⇔ EGRET
3. Advanc[d] Compton ⇔ GLAST
   (ACT,~2012) (~2006)

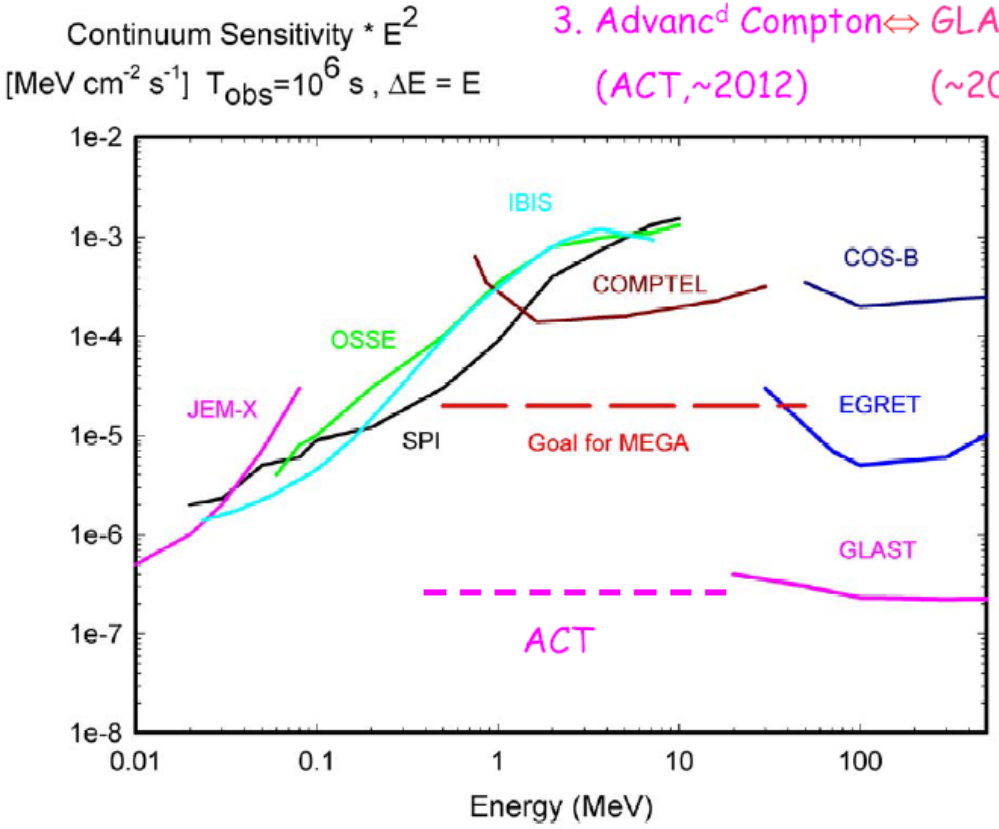

Compton Polarimetry

Compton Polarimetry

Unpolarized Beam

$$\frac{d\sigma_{KN,U}}{d\Omega} = \frac{1}{2} r_0^2 \varepsilon^2 [\varepsilon + \varepsilon^{-1} - \sin^2\theta]$$

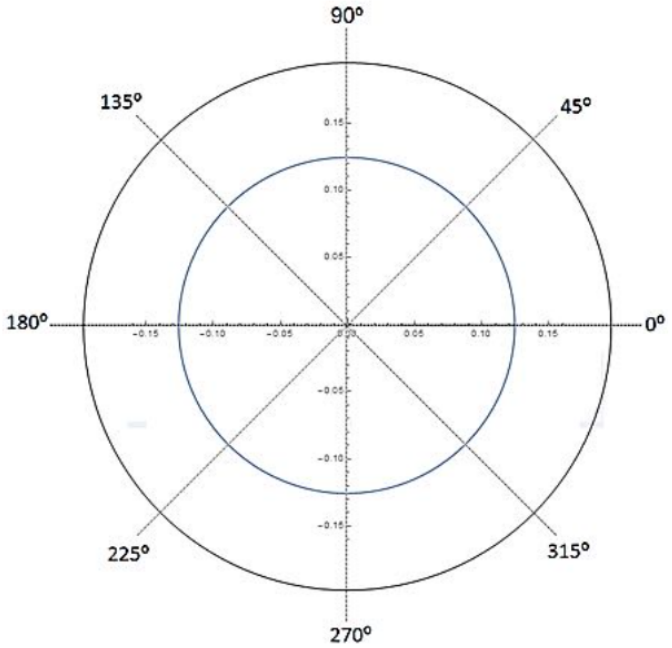

Polarized Beam

$$\frac{d\sigma_{KN,P}}{d\Omega} = \frac{1}{2} r_0^2 \varepsilon^2 [\varepsilon + \varepsilon^{-1} - 2\sin^2\theta \cos^2\eta]$$

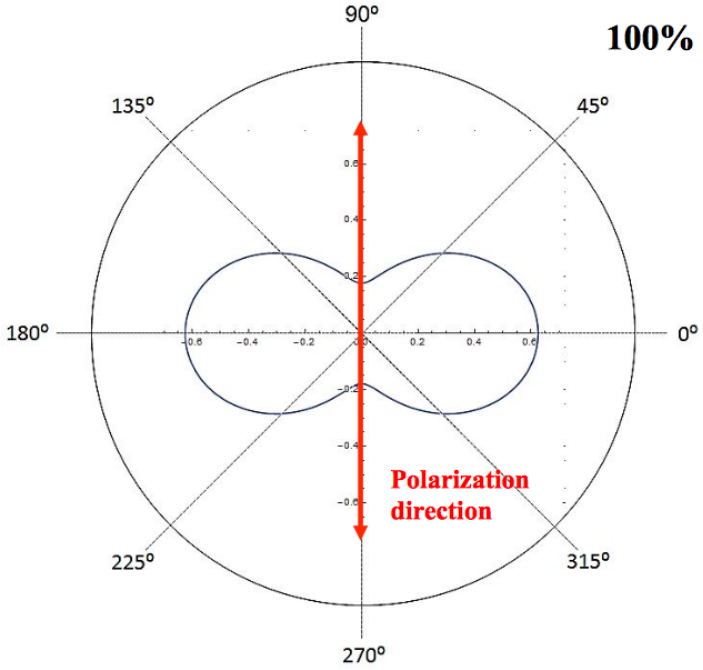

Compton Polarimetry

Compton Polarimetry

Polarization modulation factor

Klein-Nishina cross-section for linearly polarized photons:

$$\frac{d\sigma}{d\Omega} = \frac{r_0^2}{2}\left(\frac{E'}{E}\right)^2\left[\frac{E'}{E} + \frac{E}{E'} - 2\sin^2\theta\cos^2\varphi\right]$$

$$Q = \frac{N_\perp - N_\parallel}{N_\perp + N_\parallel} \qquad Q = \frac{d\sigma(\varphi = 90) - d\sigma(\varphi = 0)}{d\sigma(\varphi = 90) + d\sigma(\varphi = 0)}$$

$$Q = \frac{\sin^2\theta}{\frac{E'}{E} + \frac{E}{E'} - \sin^2\theta}$$

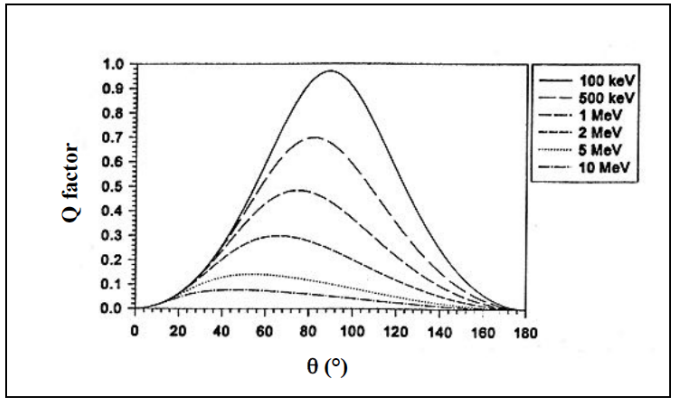

Minimum Detectable Polarization 3σ

$$MDP = \frac{4.29}{A.\varepsilon.\phi_s.Q_{100}}\sqrt{\frac{A.\varepsilon.(\phi_s + \phi_B)}{T}}$$

φ_s – source flux
φ_B – background flux
Q_{100} – polarimetric modulation factor for 100% radiation
ε – detector double event efficiency
A – detector area
T – observation time